

THE LAUNCH LOOP



A LOW COST EARTH-TO-HIGH-ORBIT LAUNCH SYSTEM

Keith Lofstrom keithl@kl-ic.com <http://launchloop.com> 2009 July 31



ABSTRACT

The Launch Loop is an Earth-surface-based launching utility that stores energy and momentum in a very long, small cross-section iron rotor loop moving at high velocity. The downward forces necessary to deflect the rotor from its otherwise straight path support a magnetically-levitated track system, control cables, and vehicles at high altitudes against gravity. This paper presents a preliminary system that can launch five metric ton vehicles to geosynchronous or near-lunar orbits at rates of up to 80 per hour.

1. A trip to Geosynchronous Orbit

You left LAX for Quito, Ecuador around 2PM yesterday, and spent the night in the Quito Howard Johnson's. Early this morning, a commuter jet brought you 3000 kilometers west to the floating runway next to JAL-Hitachi 12, the new passenger launch loop. It is the first loop powered solely by space solar power. This is your third trip this year up to High Kiev, the orbiting sports arena at GEO 35 East where you will be the ESPN camera technician for the world championship spaceball games.

Your last emergency training was only a month ago, so you walk straight to the capsule embarkation building. It is a relief to get out of the blazing equatorial sun. Your ID tag leads you to the GEO departure area and your passenger capsule. The capsule looks like a oval-shaped rowboat, with another rowboat shaped lid suspended above it. Together, they would look like a large propane tank.

The capsule has six contoured seats in a row. You climb into the first one and strap in. Four other passengers wander into the boarding area and strap in behind you. Two are fellow camera techs from other networks. Two others are newbies - one keeps asking you questions that they should have learned in training, and will be explained (again) during the pre-elevator video. Nervous. Well, so were you, the first time.

As the ground tech is checking your harness, one last passenger runs up, out of breath, pulling an airline roller-bag. No overhead bins here. Your luggage was collected from your hotel last night, and is already on its way to High Kiev. The technician glares at the late passenger. "Cargo, Quito, or into the ocean?" The late passenger gasps "Cargo". Late luggage travels cargo standby, and the loop manifest is usually full. The latecomer will be renting a jumpsuit for a day or two.

The tech makes sure that everyone is diapered and strapped in, with pockets emptied and jewelry stowed in personal pouches, then leaves with the bag. The top of the capsule is lowered and sealed. Pins slide into place. You will be sealed in this capsule, strapped to your seat, for the next 6 hours. More like a Mercury capsule than an airliner.

The seat screen comes on, with the usual boring explanation of emergency procedures. There is a jerk as your capsule is pushed into Rock and Roll, the vacuum shake chamber (at least, that is what your screen shows - there are no portholes). A loud screaming noise outside the capsule is the air leaving through massive turbo-pumps. The capsule starts shaking and bucking like a rowboat in a hurricane. This is the most violent part of the flight to orbit, while you are still on the ground. You hope they will find any leaks now, when you are only seconds away from the atmosphere, rather than in space.

A loud whistling noise outside, as air returns to the chamber. The capsule moves, gently now, and your screen shows you traveling down tracks to one of the elevator cradles. It is 11:30 A.M. local time, but the screen has changed to 1730 GMT. You wonder whether Pyotr's Restaurant will be open when you arrive. Dinner might be junk food from the concession stand. Damned time shifts. Nothing you can do now.

The capsule tilts skyward, and you are now lying on your back. There is a CLACK as it latches into an elevator cradle, and after a 10 second countdown on your screen, you are pushed into the back of your seat as the capsule starts climbing upwards. This is what 3 gees feels like - about like the kids climbing on your chest back home. Which reminds you not to bring back any more moon rocks for coming-home presents - BORING - but Megan would really like a ball signed by one of the players, so you will try to wheedle one of those.

At lift plus 17 seconds, there is a shudder, as the elevator and capsule exceed the speed of sound. Sailors on ships 3 kilometers from the west surface station will hear the crackle of a sonic boom.

The acceleration lasts only 20 seconds, but it feels longer. The acceleration slows to a gentle one-gee climb, then comes a shudder and a thump as your capsule unclamps from the acceleration cable and clamps onto the climbing cable for a three minute, 68 kilometer climb into space.

Your mind wanders to your upcoming camera work. The Polish team can get rowdy, and you want to be ready to frame a fight. Fractions of a second count, and they are counting on you to get the best action to beam to the ground, without the 250 millisecond speed-of-light delay of remotely controlled cameras.

You are moving upwards at 400 meters per second, a little over the speed of sound, and the wooshing noise outside fades away as the capsule climbs into the thin air of the upper stratosphere. There is no vibration or sense of movement; it feels like you are on the ground. Another clack as you release from the climb cable. Weight goes away as the capsule free-falls the last 8 kilometers up to west station. A newbie is vomiting into his barf bag, but thankfully the sound suppression system is working and you don't have to listen to it.

You push gently forwards into your straps as the capsule brakes to a stop. Weight returns, and the capsule rotates to horizontal again. You are on west station, 80 kilometers - 50 miles - above the surface of the ocean. You are in space, sitting in your seat, not moving. You left the ground only 5 minutes ago.

The capsule moves again, firm but smooth. There is a crunching noise below your feet, as your capsule attaches to the magnet-wing. Then another crunch, this time in back, as the apogee rocket motor is attached. Another boring announcement, and you are pushed back into your seat as the capsule is moves

briskly to the start position on the catapult. The capsule stops briefly. The newbie changes his barf bag, the other newbie taunts him, and the capsule quiets down, with only the sound of the fans. The screen shows 1738.50 GMT, and 10 seconds to launch. Your wrists and arms and head are grabbed by suction ports in your seat - you will be immobilized for the next 7 minutes.

Again, you are pushed back into your seat, as the catapult accelerates smoothly to 2.5 gees. The electronics are doing final test, and if they discover any anomalies in the magnet rail underneath, you will hear a loud siren and an emergency stop abort will slam you forward into your straps. That would hurt, but less than a reentry and an unplanned parachute trip to the ocean. That's what happens if the launch aborts later on. 6 seconds into launch, the capsule announces "main track". There is a small jolt as the catapult hands the capsule off to the rotor.

If the vehicle magnets stopped working now, the vehicle could drop onto the hyper-velocity rotor, and the capsule (and you) would be sliced in half by a stream of rotor fragments. With luck, the apogee rocket motor would fire first, propelling you out of harm's way and to a parachute reentry, saving both you and the launch loop. You've been trained to survive many things that could go wrong. They don't go wrong.

The surprise is how quiet this launch is. The fans whirl. Somebody coughs. Occasionally, a thruster fires with a snapping noise. But no loud rocket noise - that comes later, at apogee insertion. This new launch loop is missing the faint "climbing/falling chime" sound that the old launch loops made, as the magnet-wing encountered the small magnetic discontinuities in the rotor and sheath passing underneath, the pitches changing with the relative speed of each. Those wasted energy, so they designed them out.

After 5 minutes of quiet acceleration, your screen pops up "abort to orbit - 90 minutes". If anything goes wrong now, your capsule will make at least one 90 minute orbit before returning the atmosphere and re-entry. As you continue to accelerate, the time increases. At 6 minutes into launch (you started up the elevator only 15 minutes ago!) the screen flashes "abort to m288 - 78 minutes" - now the m288 maintenance station in the server sky computing belt is the closest emergency stop.

At 6 minutes and 45 seconds, the pressure eases off. You return to free fall. The capsule is now in an elliptical transfer orbit to High Kiev. You have a 5 hour and 15 minute zero gee ride ahead of you. The restraints release. You can move your head and your arms, but you stay buckled in. You call home and get the machine - everybody is at work or school. It is 1745 GMT, and 945 AM at home in Pasadena. You take a nap.

The announcement system awakes you, and you realize you've slept more than 5 hours. That was some nap - zero gee agrees with you! You dreamed of fireflies - that may have been the Van Allen radiation belt. The screen shows 2250 GMT. The apogee motor will fire in 10 minutes. The other passengers are yacking now. Nervous. The launch loop is safe, rocket motors are not. Sometimes the rocket doesn't start. That means another 5 hour descent and a high speed reentry. Then another day or two in airports getting back to the Pacific ocean launch loop for another try.

And sometimes the rocket blows up. Rather than worry, you call home - it is 2:50pm in California. Your daughter is home from grade school, and you chat about little things.

Next year, they will complete the rotating capture tether at High Houston. The ends of the tether will capture surface-direct payloads like this capsule, and also capture payloads sling-shot around the moon to make up the momentum balance. Whatever that means. You don't understand the orbital mechanics, but apparently they won't need apogee kick rockets after that. At least to High Houston.

Your thoughts are interrupted by another push into your seat, as the rocket fires. This is one of the new throttle-able solids, so thrust can be adjusted precisely to safely bring the capsule within a few hundred meters of High Kiev. After 3 minutes of rocket fire, and the last weight you will feel for days, it ceases. The screen shows the huge sphere of High Kiev floating nearby. Two tugs on long tethers float into view. The magnet-wing and the spent apogee kick motor detach with a loud ca-chunk, and one of the tugs floats out of view to recover them. The other tug grabs your capsule, and reels back in towards the station. Other tugs and capsules are floating in the distance. There will be many arrivals per hour, given the upcoming championships. Your capsule is pulled into a dock, and there is a welcome woosh outside as the dock fills with air. A vent opens, and your ears pop as the pressure equilibrates between inside and outside.

The announcement system tells you to remain buckled until the hatch cover is removed. You, and all the other passengers, ignore the announcement with a loud clicking of buckles. There is a smell of dirty diapers as you float up from your seats. It is 2330 GMT, and you've been sitting for 6 hours. Time for a shower and clean clothes. The screen shows that your suitcase arrived on a previous cargo capsule and is waiting at the hotel. And you hope the restaurant is open at midnight, so you can get something besides microwaved varenyky for dinner!

2. Introduction to the Launch Loop

Rockets are expensive. Rockets must carry enormous fuel supplies, and intricate engines that operate at high power levels for brief periods. Even with partial re-use, staging discards a lot of costly equipment. The long turn-around times for the re-usable components result in a long payback time for the initial investment, and long idle times for ground equipment. The low frequency of launches, and the differing nature of each one, require a high degree of expertise from the launch operators and increase the chance of costly, time-consuming errors.

It is difficult to imagine how larger rocket systems requiring larger facilities, longer development times, and new technologies [1] can improve the picture. Rocket launch costs will certainly improve with increased usage, but the costs may never drop low enough to make large scale space industry and space colonization practical. Alternatives to the rocket are necessary.

Proposed schemes for electromagnetic launch from the Moon [2] or Earth [3] involve very high accelerations suitable only for raw materials. The high peak power circuitry is very expensive. Orbital capture systems must be constructed from large amounts of mass already in orbit [4,5,6], or require material strengths not yet available [7].

Accelerating a vehicle to 11 km/sec (the ΔV required to launch from the Earth's surface to L5 or the Moon) at 3 gees requires an acceleration path of 2000 km. The energy necessary is modest, about 60 MJ/kg. If provided at 100% efficiency from electricity costing 12 cents per kWhr, this energy costs about

two dollars per kg. The Earth itself can be the reaction mass.

The Launch Loop [18,19] provides vehicle energy and momentum more efficiently than rockets, using simpler vehicles. The Launch Loop uses thigh speed continuous flows of materials and electronically-controlled ferromagnetic levitation. The rotor supports and drives the system with its inertia, and is segmented to eliminate axial tension. Launch Loop construction materials are commercially available in large quantities.

3. Dynamic Structures

Imagine a stream of water from a hose pointed at an angle into the sky. Neglecting air friction, the stream forms a parabolic arc, the ballistic trajectory of the individual particles in the stream. If the stream of water is moving very fast when it leaves the hose, the height of the trajectory and the distance it traverses are well beyond what can be constructed with ordinary materials. If a flat plate deflects the stream downward, the plate is forced upward. In this way, a moving stream can support a stationary weight.

If the stream is surrounded by a frictionless hose, the weight of the hose is supported by the downward deflection of the stream. When the stream reaches the ground at the end of its trajectory, it may be deflected back toward its source, and deflected forward again, completing the loop. If the hose is truly frictionless, large, apparently static structures may be built. These are called dynamic structures.

Replace the stream with an iron rotor, and the hose by a magnetic track, with a magnetic pressure of $B^2/2\mu_0$ [8]. The inertia of the iron rotor supports the structure. The rotor is deflected, but not stretched or compressed. Magnetic levitation is virtually frictionless. This allows tall structures to be built, unhindered by conventional strength-of-materials limits.

4. The Launch Loop

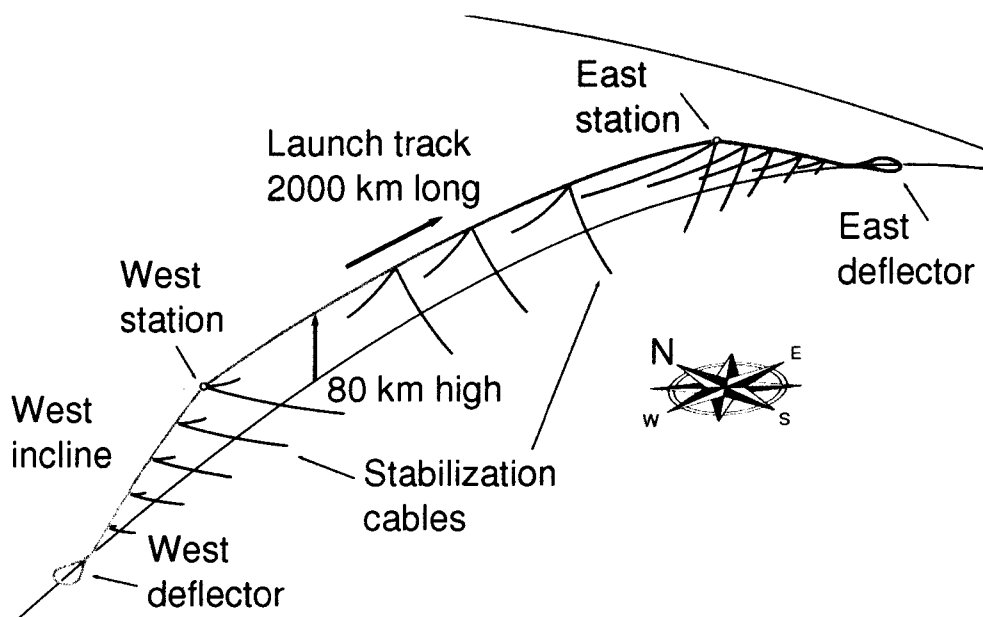


Figure 1.
Side view of the Launch Loop.
 Most cross sections are in centimeters.
 The structure is invisible from a distance.

[20]

The Launch Loop is a long, small cross-section structure built around a segmented iron rotor loop moving at 14 km/sec. The rotor is a cylinder 5 centimeters in diameter with walls 2.5 millimeters thick. This rotor circulates around the system once every six minutes, traveling around the ends, up the inclines, down the launch path, then down the incline at the other end. When the rotor reaches the far end of the Launch Loop, it is deflected 180° and returned to complete the cycle.

Large forces are required to deflect the moving rotor. These forces support a *stationary* track system of cables, control electronics, and permanent magnets by ferromagnetic attraction.

At the top of the Launch Loop is the 2000-km long launch path. Vehicles riding magnetically on the forward rotor of the launch path are accelerated at 3 gees to reach ground-relative transfer orbit velocities up to 10.5 km/s. Small payloads may be pushed faster.

The launch path track is suspended on permanent magnets one centimeter below the iron rotor. The launch path track supports sensor and control electronics packages, as well as parachutes to protect sections of track from catastrophic system failure. The rotor and static track structure of the launch path weigh about 3 kg/m and 7 kg/m respectively, and are shown in Figure 2.

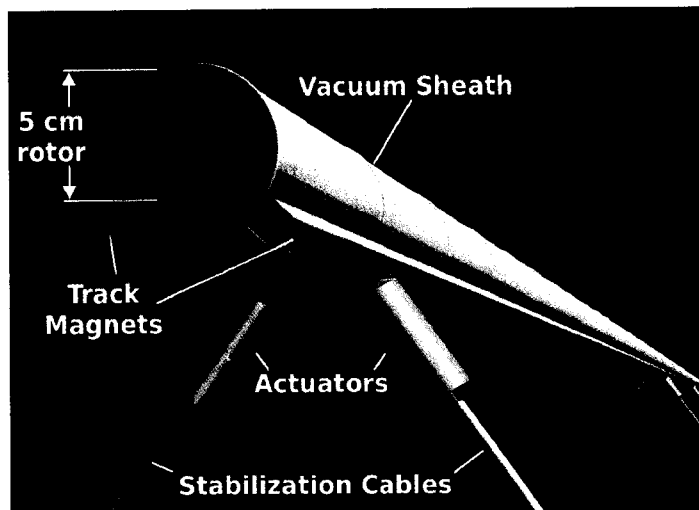


Figure 2.

A cross section of the rotor and track.

Actual surfaces will be black for high thermal emission

In front of and behind the launch path are the inclines, which slope down to the surface at angles of 9 to 20 degrees. The forward and reverse rotors of the inclines are surrounded by lightweight vacuum sheaths. The sheath will get very hot. There may be “side wings” that help with black-body radiation, and also act as meteor bumpers. Electronics packages and other temperature sensitive gear will hang some distance below the track.

The inclines are much heavier than the launch path track. Anchor cables control the sections against wind, and the track must support an airtight sheath and vacuum pumps. To compensate for the extra weight, the inclines curve more than the Earth's surface. The tension on the inclines is relieved by diagonal cables to the surface.

The inclines and the launch path are joined by two curved, 5000-metric-ton deflector sections containing

magnets, control systems and elevators from the surface. The upper deflectors are referred to as the "east" and "west" stations; vehicles are hauled up to west station and launched from there.

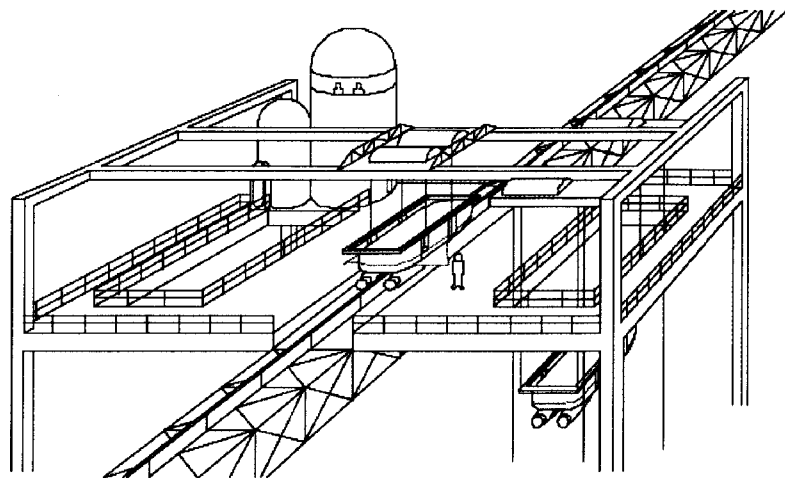


Figure 3.

West station, showing a vehicle being loaded onto the track.

Old drawing, needs updating

The long elevators to the stations are supported by pulleys from the anchor cables. The vehicles are brought up these cables rather than up the west incline to simplify the spacing controllers on the incline. Other benefits of this approach are minimized incline weight, shorter upward transit times, and less likelihood of sheath damage.

Near the Earth's surface, each incline ends at a curving ramp with magnets that deflect the rotor to or from the horizontal plane. Once the rotor is horizontal, it is twisted on its length axis 90° so that the broad surface points at the horizon. The rotor is then deflected 180° in the horizontal plane by a large, flat semicircular section (14 km radius) of high-energy magnets. The windings for the linear motors that drive the rotor are positioned between the semicircular sections and the upwards ramp on the east end. The rotor is then twisted back to flat, and sent back west through the system to complete the loop. The east end of the Launch Loop is shown in Figure 4.

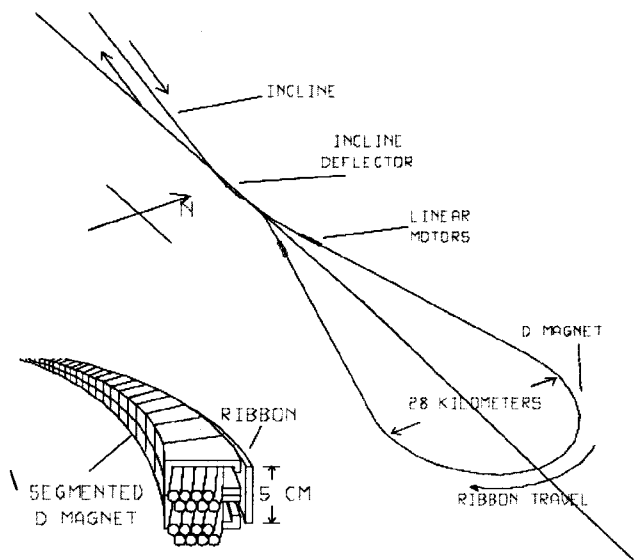


Figure 4.

The east end deflectors, motors, and the start of the east incline.

The inset shows a section of deflector magnet.

Old drawing, for a flat rotor - needs updating

Tfew multiplies and additions at a 340 kHz sample rate, easily handled by modern digital signal processors.

Central host computers program the controller look-up tables and multiplication constants over communication buses. These constants are computed from the state of the Launch Loop system, including controller failures. There are approximately 150 km of D magnets in the Launch Loop system; 150,000 of these controllers are needed.

Each one-meter control section must handle 30 kW peak, which should cost about what a 6 kW continuous switching power supply would cost in very large quantities. Prices of \$0.10 per average watt are common for tested and installed controllers. The digital controller and sensors may cost \$200, for a unit controller cost of \$800.

10. Low Acceleration Sections

he Launch Loop is located on the equator to minimize vehicle apogee ΔV as well as weather and Coriolis effects. For safety and ease of construction, the system is located over the equatorial ocean, far from land. This means increased shipping costs from northern hemisphere industry, increased corrosion, and long anchoring cables to the deep sea bed. These drawbacks are balanced by the ability to deploy the Launch Loop from a relatively flat surface, and move the various deflectors during construction. Much of the system will be submerged to avoid winds and surface currents.

While launch loops can be placed in the Atlantic and Indian oceans, some of the best sites in the equatorial Pacific ocean, south of the west coast of the United States.

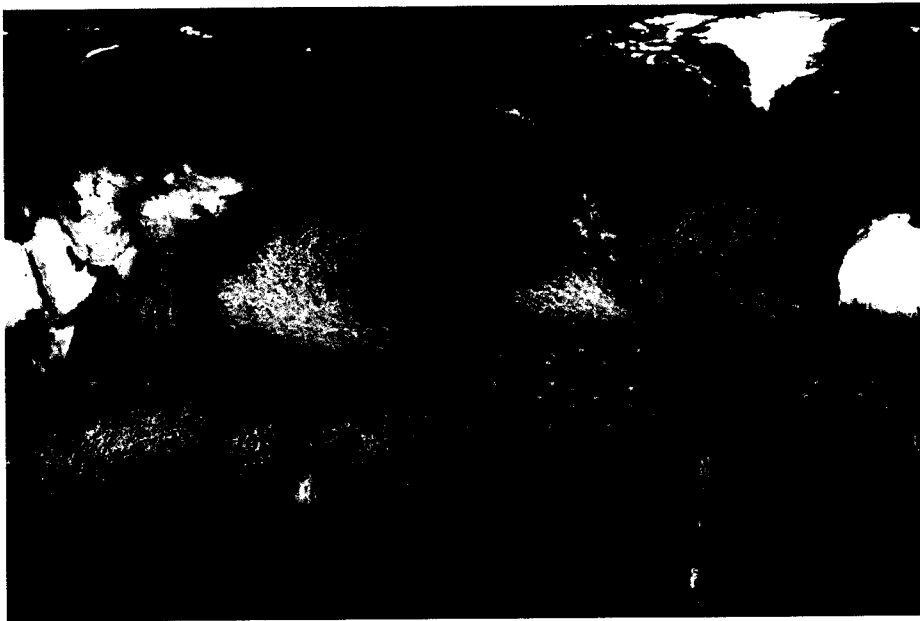


Figure 5:

A map of historic typhoons and hurricanes, and some possible Launch Loop sites where storm activity is low and predictable.

Floating sites anchored above oceanic mountains will reduce undersea cable costs. Many promising sites are located near Kirabati, Jarvis Island, and Howland Island south of Hawaii, eastward to seamounts

northwest of the Galapagos Islands. Since many of these islands are sensitive ecological preserves, it will not be prudent to anchor to them, nor locate airstrips and land-based infrastructure on them. Launch Loops should be anchored far enough apart that the failure of one will not affect others. Launch loops should not be located directly on the equator, where future technology may permit the construction of space elevators. And they should not be up-range or down-range of the Kourou Space Launch Center, at 5 degrees north on the east coast of South America. Even with these restrictions, there are sites for hundreds of Launch Loops. Since very large diameter, large-mass, high throughput Launch Loops may be constructed, there is room to launch millions of tons per hour into space.

The sloping sheath and cables are subject to wind loading in the lower atmosphere, although most of the system is in near vacuum. The sudden loads caused by wind gusts cause extra stress on the structure, and the static loading of steady winds distort the structure and contribute inaccuracies to vehicle trajectories.

Assuming a drag coefficient of 0.5, a 100-knot sea level wind places a 50 N/m load on a 10-cm-diameter sheath, as would a 200-knot wind at the 250-mbar level of the atmosphere. A sheath with a rotating airfoil shape may cut the drag coefficient by a factor of 10 or more.

Equatorial winds tend to be unpredictable and vary greatly with altitude [12], but their maximum speeds are relatively low and the lack of Coriolis force inhibits cyclones. The most severe stresses can be expected during squalls, whose maximum winds cannot be forecast with present techniques. The equatorial site should be chosen with measured wind history in mind, so that the system survives normal storm conditions.

5. System Deployment

The Launch Loop is assembled floating on the surface of the ocean, at rest. Deployment imposes some of the most severe stresses on the system, as the launch track is now on the surface and must be protected by a temporary sheath that can stand off a full atmosphere. In addition, the control system must compensate for ocean wave forces. During this time, the system may be started with additional deployment magnets and linear motors above or below the rotor/track to until the rotor is at full speed.

The rotor is started, slowly at first, by pulling on it with motors at the ends of the Loop. Given the enormous inertia of the rotor, and the weak joints that separate the rotor segments, the initial acceleration is about 1 cm/sec². At this acceleration, it takes 9 hours just to make one pass of the rotor through the motors, and 3 days before the motors can work at full power.

The rotor weighs 15,600 metric tons; accelerating it to 14 km/sec requires 1.5E15 Joules of kinetic energy. If this energy is put in at a 300 MW rate, the system requires 60 days to reach full speed, while the Loop is flat on the surface. For a Loop operation at this power level, it may be practical to temporarily attach 1 GW of gas turbines on floating barges to accelerate the rotor to full speed more quickly.

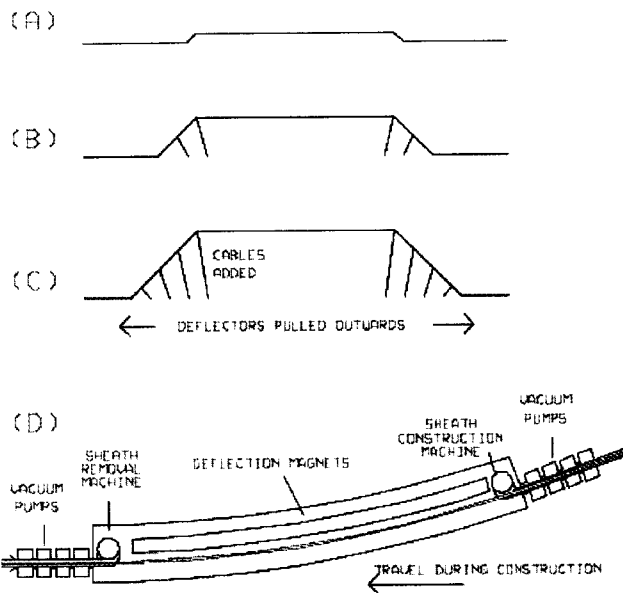


Figure 6. Deploying the Launch Loop.

(a) up to speed, flat on the surface.

(b) partially raised, with the ramps pulling towards the ends.

(c) fully deployed, the track sheath being stripped away.

(d) the west end incline deflector during deployment.

The deployment process is illustrated in Figure 6. Before deployment, the east and west stations are near the surface. The deflection ramps are temporarily pulled 300 km inwards, and are located next to the stations, temporarily supported on barges. When the system is up to speed, the stations are raised off the barges by increasing the curvature of the surface incline deflectors and the tension in the station anchor cables. The rotor is now being deflected 5 degrees at the incline deflectors and at the station; the distance from incline bottom to station top is 100 meters.

The system is brought to altitude by slowly drawing the surface incline deflectors away from the stations. New sheath is built around the slowly-growing inclines and removed from the long sections between the inclines and the end deflectors. Stabilization cables are added to the inclines. If automatic construction machinery is capable of producing 20 meters of sheath per minute, the deployment process should take about 10 days.

When the system finally reaches 80 km altitude, the temporary sheath is cut away along the entire length of the launch track. Segments of the temporary sheath sections are lowered down the station cables. The launch track stabilization cables are tightened to make up for the lost weight of the sheath.

6. Dynamics of the High Speed rotor

The rotor will be analyzed assuming a uniform weight per length m_r , without tensile or bending forces. Lower case m is used for distributed masses, while upper case M is used for point masses. A rotor moving at a speed of V_r may be deflected by an angle θ with a force of:

$$(1) F = 2 m_r V_r^2 \sin(\theta/2) \approx m_r V_r^2 \theta$$

The rotor speed does not change; just the direction of the velocity vector.

A distributed force can deflect the rotor as well. For example, a rotor constrained to follow the curvature of

the Earth requires a distributed force to hold it to the curved path. If the rotor is moving at circular orbital velocity, the deflection force is equal to its weight. If it is moving faster than orbital velocity V_o , deflecting it to follow the curve of the Earth requires an external downward force per length of

$$(2) \quad f = a_g m_r \left(\left(\frac{V_r}{V_o} \right)^2 - 1 \right)$$

The east-bound surface-relative orbital velocity at 80 km altitude is about 7400 m/s. A rotor moving at a surface-relative velocity of 14 km/s and weighing 3 kg/m requires an external downwards force of 68.5 N/m. This force can be provided by the weight of a non-moving track weighing 7.1 kg/m. The same rotor moving retrograde can support 5.9 kg/m of stationary track.

The Launch Loop rotor is constrained to rise and fall as it travels around the system, changing altitude by 80 km in the process. The rotor moves faster at ground level because it is accelerated by gravity on the way down from 80 Km and decelerated on the way up. The higher ground velocity of 14,055 m/s requires the rotor to stretch by 0.4%. The mass density is lower by the same amount. To accommodate this stretch, the rotor may be constructed out of two-meter-long segments connected with sliding joints.

The axial acceleration of the rotor requires large amounts of force and power. If the rotor velocity is increased by ΔV , the necessary force is:

$$(3) \quad F = m_r V_r \Delta V$$

A 14 km/s, 3 kg/m rotor is slowed 3.6 m/s by a force of 150 KN. This force can be used to accelerate a 5000-kg space vehicle at 3 gees. Force is provided purely by the deceleration of the rotor, and does not necessarily result in any stress on the rotor.

The power evolved by decelerating the rotor is given by:

$$(4) \quad P = m_r V_r^2 \Delta V$$

For the same 3.6 m/s slowdown, the power is 2.1 GW. Part of this power is turned into payload kinetic energy, and part of it appears as waste heat in the rotor.

7. Magnetic Deflection of a Moving rotor

The rotor may be coupled to the track by ferromagnetic attraction or eddy current repulsion. Ferromagnetic attraction is the well known attraction between magnets and iron. Eddy current repulsion is based on the diamagnetic properties of moving conductors.

Eddy currents are produced by changing the magnetic flux through the rotor. These currents force the flux out of the rotor and generate repulsive forces. Eddy current repulsion is being considered for some magnetic levitation train designs [8] because the system is more stable and the track is cheaper.

Eddy current repulsion's main drawback in launch loops results from the limited conductivity of elevated

temperature conductors. Aluminum has the best conductivity per weight of any normal metal, but the high currents necessary to generate lift result in resistive losses of hundreds of watts per meter. This results in an unacceptably large standby dissipation for the Launch Loop.

Ferromagnetic attraction is unstable, but this problem can be masked electronically. A control winding can also compensate for vehicle-induced transients. With a spacing of 1 cm, one may expect a magnet lift-to-weight ratio of 3 or better. The control winding dissipation is minimized by using permanent magnets, but some power is lost correcting perturbations. If the winding power is 80 mW/N in the track and 15 mW/N in the semicircular deflectors and the east and west stations, the power dissipated in the windings is 35 and 90 MW respectively. Variations of the track magnetic field also induce currents and drag in the rotor.

8. Stability of a Magnetically Deflected Rotor

Attractive magnetic levitation is unstable. If the current to the electromagnet inducing the magnetic field is constant, moving the levitated body closer to the magnet decreases the gap, resulting in an increased magnetic field. The increased field results in increased force, accelerating the levitating body towards the magnet even faster. In the Launch Loop, this instability is corrected by electronically controlling the winding currents in short segments of the deflector magnet.

The D deflector magnets at the ends of the Loop pose the most difficult control problem. With a rotor speed of 14 km/s, and a deflector radius of 14 km, the rotor deflection acceleration is $14,000 \text{ m/s}^2$, or 1430 gees. With a 1 mm nominal gap between the magnet and the rotor is, a perturbation of only $1 \mu\text{m}$ results in a perturbation acceleration of 28 m/s^2 , which increases the perturbation still further. Thus, perturbations double every 180 microseconds, or every 2.5 meters of travel around the deflector.

Over shorter distances, the rotor can buckle. The rotor stiffness resists perturbations with wavelengths less than 30 cm, but longer wavelength perturbations grow exponentially. This "stiffness wavelength" determines the number of control points per meter, while the perturbation growth time determines the time sample rate. If the perturbations grow slowly, the same control values may be shifted to many succeeding controllers, saving computational hardware and providing numerical redundancy.

Both these effects are driven by the variation of the magnetic field with gap spacing g , which is given by:

$$(5) \quad B = \frac{\mu_0 I}{2g}$$

μ_0 is the permeability of free space, I is the effective current in the electromagnet winding in amp-turns, and g is the gap in meters. The flux passes through the gap twice, into and out of the rotor. The magnetic pressure $B^2/2\mu_0$ produces an attractive force between the two poles of the magnet and the iron rotor of:

$$(6) \quad f = \frac{W_p B^2}{\mu_0} = \frac{W_p \mu_0 I^2}{4g^2}$$

where W_p is the width of the magnet pole. The rotor has a mass per length of m_r , resulting in a magnetic centrifugal acceleration of:

$$(7) \quad a = -\frac{W_p \mu_0 I^2}{4 m_r g^2}$$

With a nominal rotor-to-magnet gap g_0 and the correct control current I_0 , the magnetic centrifugal acceleration is $-a_0$, equal to the centrifugal acceleration of the rotor around the deflector.

$$(8) \quad a_0 = \frac{W_p \mu_0 I_0^2}{4 m_r g_0^2}$$

Assume a fixed deflector (not always a good assumption!) and small perturbations \hat{z} from nominal gap g_0 . This calculation is performed in a moving frame of reference $\hat{x} = x - V_r t$ following the rotor. The change in centrifugal acceleration with gap is given by:

$$(9) \quad \frac{\partial a}{\partial \hat{z}_r} = \frac{W_p \mu_0 I^2}{2 m_r g^3} \approx \frac{W_p \mu_0 I_0^2}{2 m_r g_0^3} \approx \frac{2 a_0}{g_0}$$

By a similar argument, the acceleration changes with control current as

$$(10) \quad \frac{\partial a}{\partial I} \approx -\frac{2 a_0}{I_0}$$

The acceleration is simply the second derivative of \hat{z}_r . For small perturbations, the local equation of motion is thus:

$$(11) \quad \frac{d^2 \hat{z}_r}{dt^2} = \left(\frac{2 a_0}{g_0} \right) \hat{z}_r$$

which has solutions of the form:

$$(12) \quad \hat{z}_r = \hat{z}_{r_0} e^{\pm(t/\tau)} \quad \tau \equiv \left(\frac{g_0}{2 a_0} \right)^{\frac{1}{2}}$$

The doubling time for the perturbation is $\tau \ln 2$. If the stiffness of the rotor in the \hat{x} direction is included, a more complex picture emerges. The stiffness introduces the bending force f_b :

$$(13) \quad f_b = -E_{FE} I_b \frac{\partial^4 \hat{z}_r}{\partial x^4}$$

E_{FE} is Young's modulus for the iron rotor, and I_b is the bending moment, which is given by:

$$(14) I_b = \frac{\pi}{4}(R_o^4 - R_i^4) \approx \pi th R^3$$

for a flat rotor with an outer radius of R_o and an inner radius of R_i . This can be approximated with the average radius R and thickness th . For a 3 kg/m iron rotor (density = 7.874 gm/cm³) with a diameter of 5 cm, $th = 2.4$ mm and $I_b = 1.19E-7$ m⁴.

The mass of the rotor is given by $m_r = 2\pi\rho_{FE} th R$. The longitudinal speed of sound in the material is:

$$(15) C_{FE} \equiv \left(\frac{E_{FE}}{\rho_{FE}} \right)^{\frac{1}{2}}$$

For iron, $C_{FE} = (211E9/7874)^{1/2} = 5177$ m/s. The acceleration, which is the force divided by the mass, is given by:

$$(16) a_b = - \left(\frac{C_{FE}^2 R^2}{2} \right) \frac{\partial^4 \hat{z}_r}{\partial x^4}$$

The differential equation describing the rotor is thus:

$$(17) \frac{\partial^2 \hat{z}_r}{\partial t^2} = \left(\frac{2a_0}{g_0} \right) \hat{z}_r - \left(\frac{C_{FE}^2 R^2}{2} \right) \frac{\partial^4 \hat{z}_r}{\partial x^4}$$

This equation can be solved with Fourier analysis. Assume that:

$$(18) \hat{z}_r = \hat{z}_{r_0} e^{i(\omega t - kx)}$$

where ω is the angular frequency and k is the wave-number, related to the wavelength by $k = 2\pi/\lambda$. Equation (17) reduces to:

$$(19) -\omega^2 = \left(\frac{2a_0}{g_0} \right) - \left(\frac{C_{FE}^2 R^2}{2} \right) k^4$$

For $k = 0$, equation (19) implies the growth time of equation (12). As k gets larger (or equivalently, the wavelength gets shorter), the imaginary quantity ω tends towards zero as the growth time gets larger. For short wavelengths, ω is real and the solutions resonate, but do not grow with time. The system is stable, and dispersive; wave packets on the rotor spread out over time.

Since $\lambda = 2\pi/k$, the condition of stability becomes:

$$(20) \lambda < 2\pi \left(\frac{g_0 C_{FE}^2 R^2}{4 a_0} \right)^{1/4}$$

For $C_{FE} = 5177 \text{ m/s}$, $g_0 = 0.01 \text{ m}$, $R = 0.25 \text{ m}$, and $a_0 = 9.81 \text{ m/s}^2$ equation (20) yields a wavelength of 144 cm. Sampling theory suggests the control sections should be no longer than half this wavelength, or about 70 cm. The filtering job is easier if the sections are smaller still, perhaps 40 cm long.

9. The D Magnet Digital Controller

What magnitudes of currents and voltages must the controller handle? This is dependent on the size of the perturbations, of course; if the system is well behaved, they are zero. Control sections can fail, however, and introduce perturbations as large as the limits of their control range. Thus, the larger the control range, the more control range is needed to correct. This is not a problem if the percentage of failed sections is kept small.

Assume a sinusoidal variation in spacing moving with the rotor, with an amplitude of $\pm 100 \mu\text{m}$, and a wavelength of 0.4 m. From equation (10), the peak control current is $0.1 I_0$. The voltage can be computed from the change of energy and thus the flow of power in and out of a local section of magnet:

$$(21) \quad V I_0 = \text{Power} = \frac{\partial E}{\partial t} = V_r k f z$$

where z is the amplitude of the variation and f is the magnet force. The instantaneous power in a 10 cm section of magnet, for half the rotor, is 15 kW. The local controller is handling 10% of the power. The rest of the power is handled by the main magnet controller. 1500W per controller is quite a bit; while the controllers need not dissipate this much power continuously, they must be able to stand off this voltage-current product. Many semiconductor devices are able to stand pulse currents that are some multiple of their DC rating. These devices handle high-current pulses less than 100 microseconds long; devices with DC power ratings of 300 watts are probably adequate.

The control range allowed by the local controllers lets them correct a perturbation of up to $0.1 g_0$, or $\pm 100 \mu\text{m}$. This amount of perturbation can be caused by the preceding 4 meters of control section being stuck on (40 control sections), or by an uncorrected perturbation of $2 \mu\text{m}$ up to 7 meters away. The preferred failure mode for a controller is off, rather than stuck on. Current limiting shutdown circuits and fuses achieve this.

20 separately switched and fused control sections (10 for each side of the rotor), each 10 cm long, make up a single one-meter-long control block. Each control block has its own group of optical position measurement stations and its own digital processor. The measurement and control process performs only a The incline sections and launch track support only their own weight, and deflect the rotor more gradually than the D magnets at the end of the Launch Loop. The lower forces and wider spacings involved allow widely spaced track controllers that use less power than their equivalents on the D magnets. Unlike the D magnets, however, the track is not solidly anchored to the ground, and is far lighter. This results in a more complex mathematical description. The absolute position of the track is harder to determine since it is much farther from any fixed reference. This requires high accuracy measurements of very long paths. With laser interferometers measuring lunar distances to millimeters, 80 kilometer measurements to 10s of

microns is not a hopeless task.

There are two z values to account for; z_r for the rotor and z_s for the horizontally stationary track. The stiffness of the track is important, and due to its complicated nature, is harder to compute. The track is under tension, which adds terms to the descriptive equations.

Define z_r as the deflection of the rotor from nominal position, and z_s as the difference between normal and perturbed track position. The track and rotor are normally spaced about 1 cm apart. The position in the moving frame is \hat{x} , where:

$$(22) \quad \hat{x} = x - V_r t$$

The z position of the rotor in the moving frame is \hat{z}_r .

The forces pulling down on the rotor are:

$$(23) \quad f = -m_r \frac{\partial^2 \hat{z}_r}{\partial t^2} - EI_r \frac{\partial^4 \hat{z}_r}{\partial \hat{x}^4} - \left(\frac{2f_0}{g_0} \right) (z_r - z_s)$$

The left hand side of the equation is the distributed "control force" that the controller manipulates by controlling magnet voltage and current. The first right-hand term is the kinematic term, and rotor bending is accounted for by the second right hand term, where EI_r is the rotor stiffness. m_r is the rotor mass-per-length.

The third right-hand term is the magnet instability term. g_0 is the nominal rotor to track spacing, while f_0 is the nominal force per length. The characteristic time $\tau \equiv \sqrt{g_0 m_r / 2f_0}$ is much longer than the τ of the D magnets; 30 milliseconds versus 180 microseconds. This means the controllers can be slower and spaced further apart.

Equation (23) can be expressed in fixed-frame coordinates as:

$$(24) \quad f = -m_r \left(\frac{\partial^2 z_r}{\partial t^2} - 2V_r \frac{\partial^2 z_r}{\partial x \partial t} + V_r^2 \frac{\partial^2 z_r}{\partial x^2} \right) - EI_r \frac{\partial^4 z_r}{\partial x^4} - \left(\frac{2f_0}{g_0} \right) (z_r - z_s)$$

The track position equation is similar, but includes a tension term as well:

$$(25) \quad f = m_s \frac{\partial^2 z_s}{\partial t^2} + EI_s \frac{\partial^4 z_s}{\partial x^4} - \left(\frac{2f_0}{g_0} \right) (z_r - z_s) - T_s \frac{\partial^2 z_r}{\partial x^2}$$

The force is determined by the magnet controllers in the track. A typical track control equation is:

$$(26) \quad f = m_r (a_{rs}(z_r - z_s) + a_s(z_s))$$

Where a_{rs} is a function of the position difference of the rotor and track, while a_s is a function of

absolute position of the track only.

Measuring the absolute track position is more costly than measuring the difference position, requiring some form of laser interferometry. The functions should be chosen so that the a_s function is sampled far less frequently than the a_{rs} function.

Making the substitution $z = z_0 e^{i(\omega t - kx)}$, the above equations may be Fourier transformed:

$$(27) \quad f = (m_r(\omega - V_r k)^2 - EI_r k^4) z_r - \left(\frac{2f_0}{g_0} \right) (z_r - z_s)$$

$$(28) \quad f = (-m_s \omega^2 + EI_s k^4 + T_s k^2) z_s - \left(\frac{2f_0}{g_0} \right) (z_r - z_s)$$

$$(29) \quad f = m_r (a_{rs}(\omega, k)(z_r - z_s) + a_s(\omega, k)z_s)$$

The mass ratio of the track to the moving rotor is defined as $\mu \equiv m_s/m_r$. The magnet non-linearity term is simplified with $\alpha_0 \equiv 2f_0/g_0$. The $V_r k$ term is replaced by $\omega_k \equiv V_r k$. Unless k is very large (that is, a very short wavelength) the bending terms can be ignored. The tension term modifies the character of the solution only slightly, so it is ignored for now. The above equations are further reduced to:

$$(30) \quad a_{rs}(z_r - z_s) + a_s z_s = (\omega - \omega_k)^2 z_r - a_0(z_r - z_s)$$

$$(31) \quad a_{rs}(z_r - z_s) + a_s z_s = -\mu \omega^2 z_s - a_0(z_r - z_s)$$

The following relation between z_r and z_s can be derived:

$$(32) \quad z_r = \frac{\mu \omega^2}{(\omega - \omega_k)^2} z_s$$

Equations (31) and (32) are combined, and the z_s term factored out:

$$(33) \quad \frac{a_{rs} + a_0}{a_s + \mu \omega^2} = \frac{(\omega - \omega_k)^2}{\mu \omega^2 + (\omega - \omega_k)^2}$$

Equation (33) is the characteristic equation for the track section. Since a_0 is not precisely known, and the a_{rs} term is a function of imperfect measurements, there is always a residual non-zero value for the left side of the equation. For large ω_k , equation (33) can be solved for four real roots, indicating solutions that propagate down the system, to be removed at a ground cable actuator. Unfortunately, as ω_k becomes small (or the wavelengths become large), two of the roots split and asymptote towards the complex poles defined by

$$(34) \quad \omega_p = \frac{1 \pm i\mu^{half}}{\mu+1} \omega_k$$

One of the poles is unstable; unless the left-hand side of equation (33) is exactly zero, or the proper a_s and a_{rs} are chosen, long-wavelength perturbations grow with time as they propagate down-rotor.

The problem is that the left side of equation (33) scales differently with ω_k than the right hand side, but this can be corrected with proper measurement and control. Damping factors can also be added to the control equations, making it possible to actually damp out perturbations. However, the damping factors must be chosen so that the measurements they depend on are possible to make. Acceleration measurements are easier and cheaper to make than absolute (ground based) position measurements.

One choice for control equations is:

$$(35) \quad a_{rs} \equiv \gamma \mu \omega_k^2 + c_1 \omega_k i + c_2 \omega_k i$$

and

$$(36) \quad a_s \equiv a_0 \left(\frac{\omega}{\omega_k} \right)^2 + c_4 \omega_k i$$

where γ is an arbitrary constant which determines the placement of the real part of the four roots of the system. If $\mu=2$, a good choice for γ is 0.05. c_1, c_2 , and c_4 are small constants chosen to make small, positive imaginary parts for the four roots. The $(\omega/\omega_k)^2$ term can be computed from sensitive accelerometer measurements without having to perform a numerically noisy double differentiation of an absolute position measurement.

Define $\xi \equiv \omega/\omega_k$, the normalized ω . There will be 4 roots for this fourth order system. Further define the function $f(\xi)$ as:

$$(37) \quad f(\xi) \equiv \frac{\xi^2 (\xi-1)^2}{\mu \xi^2 + (\xi-1)^2}$$

A plot of $f(\xi)$ will show double zeros at $\xi = 0$ and $\xi = 1$, and a local maxima in between.

γ should be chosen between the local maxima and zero. If we set $\gamma = f(\xi)$, we will get four real roots in ξ . These will be the real parts of the normalized roots of the system. If the imaginary parts of the roots are small compared to the real parts, equation (37) may be approximated by:

$$(38) \quad f(\xi) \approx \gamma + \frac{\partial f}{\partial \xi} \Delta \xi$$

Using equations (33) through (38) and ignoring some small terms, we arrive at the following equation for the small imaginary parts of the roots:

$$(39) \quad \Delta \xi \approx \frac{i\omega_k}{\frac{a_0}{\gamma} + \mu\omega_k^2} \frac{c_1\xi + c_2 - \gamma c_4/xi^2}{\frac{\partial f}{\partial \xi}}$$

There are four $\Delta \xi$, one for each real root ξ . The control constants c_1, c_2 , and c_4 may be chosen for robust, positive imaginary parts.

Other control functions are possible as well. The functions described here demonstrate that real-world solutions are possible, and give an idea of their complexity.

Knowing the approximate nature of the linear section controllers, their computational complexity can be determined. Assume the controllers are spaced 10 meters apart, and compute new control values for each two meter section every millisecond, for two sides of the rotor. Assume the control algorithm involves 5 multiplies and adds for a fourth-order differential equation in time and second-order in space. Each controller has 20 microseconds to do a multiply-add, which can be performed with a very simple serial architecture integrated circuit. 520,000 of these circuits are needed.

Power levels for the track-rotor system are difficult to compute. As the area disturbed by the vehicle passes a section of track, the magnetic field, and the energy stored in it, must change. A rapid change in energy implies a large flow of power through the magnet control electronics. The magnitude of this burst of power, and its duration, determine the power rating necessary for the controller.

The passage of dc magnets on the vehicle past stationary windings on the track can also be used to power the spacing control magnets. Such schemes for reducing the power level in the spacing controllers must be both fail-safe and cheap.

The magnetic field in the disturbed region tends to propagate to the front or the disturbed region, carried along by the induced currents in the rotor. The amount of this propagation is determined by the design, and determines how much extra field must be provided by the control electronics, and how much they cost.

The most magnetic force is needed when the vehicle is about to leave the rotor and is moving about 11 km/s in relation to the track. The magnetic energy stored in the gap between rotor and track must increase by 25 Joules per meter. Some of this energy is "pulled along" by the rotor and some must be provided by the track control coils. With about 2 milliseconds to provide the energy, high controller power is needed.

At the other end of the disturbance region of the track-rotor system, the field energy must be drained away and the spacing forces restored to normal. Again, a high power rate may be needed, unless the energy in the track-rotor system is made to propagate at the same speed as the vehicle.

Assume that the disturbance is made to propagate with 80% efficiency. The electronic devices in the controllers must handle 5 Joules per meter in 2 milliseconds. 2500 watts of peak-power handling is needed per meter. This is equivalent to about 1000 watts per meter of DC device power rating, or about \$100 of power handling controllers per meter of system track.

Only the last 500 km of track require expensive, high-power controllers. This section of track has the

highest energy rate-of-change, because the vehicle moves fastest and needs high hold-down forces here. The rest of the track can be made with the same low-power controllers used by the westbound rotor.

An alternative that may reduce this peak energy is a series of spring loaded “cock and release” counterweights hanging below the track. These may be able to rapidly change the vertical motion of the track during a vehicle passage, requiring less work from the spacing controllers.

11. Rotor Design for the Launch Loop

The core of the Launch Loop is the rotor; its properties control the design of the rest of the system. The rotor is made with sliding segments to prevent tension from building up in the structure.

Necessary rotor properties include:

- High electrical resistance path for high drag during vehicle launch.
- Low circumferential electrical resistance for linear induction motor currents.
- $\pm 3\%$ stretch allowed by expansion joints.
- Tolerance of vibrations generated by vehicle magnets.
- Tolerance of temperatures up to 1000K .
- Low sputter/spalling yield outer surface.
- High infrared emissivity for cooling.
- High permeability path for deflection magnet flux.
- High stiffness perpendicular to the plane of the rotor, to minimize flexing, and thus the number of control sections in deflection magnets.
- Hypervelocity disintegration into small fragments if the launch loop fails, allowing complete burn-up in the ocean or atmosphere
- High axial strength, when extended, to speed rotor start-up.
- Inexpensive manufacture from common materials.

The present design assumes a rotor constructed with 2-meter-long segments separated by sliding joints. The segments may be made from flat laminations of transformer iron separated by high-temperature insulation. A typical segment joint is pictured in Figure 7. A complete Launch Loop uses 2.6 million of these segments.

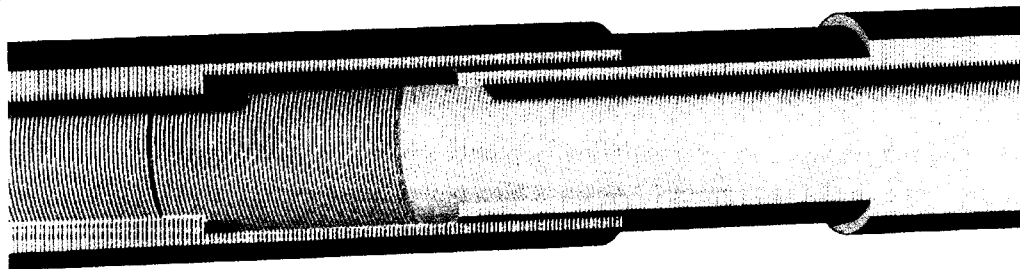


Figure 7. Joint for a 2 meter rotor segment. The core may consist of laminated iron, or a weave of iron wire. The surface is smooth carbon to minimize sputtering.

Another promising approach involves a rotor made from woven iron wire. The wire may be woven to increase the penetration of magnetic fields into the rotor, yet provide low resistance paths for the drive motor. The wire loops in such a scheme have a characteristic wavelength, and systems of alternating magnets with different pole spacings will see different effective impedances. This allows the vehicle magnets to see a much higher impedance than the linear induction drive motors do, providing for high vehicle accelerations. It may be difficult to stiffen such a rotor against bending, however.

12. Anchor Cables and Structural Shape

The Launch Loop is supported by the deflection of the moving rotor; its shape is maintained by weights and anchor cables. The long cables are tapered, and thicker at the top than at the bottom, for a constant stress per area. This allows the use of presently available materials. The characteristic length (or support length) H_c of the cable material is defined as $H_c \equiv Y/a_g \rho$, where Y is the strength per area, a_g is the gravitational acceleration, and ρ is the density. Kevlar™ fiber yarn has a tensile strength of 2.7 gigapascals, and a density of 1440 kg/m³ [9], for a raw characteristic length of $H_c = 191$ km. The Kevlar cables used here are 40% epoxy-fill by weight, and have a safety factor of 1.5, resulting in a characteristic length of $H_c = 80$ km.

The long cables run diagonally to the ground. Due to their gradual taper, they follow a modified catenary curve, not the standard cosh() function. The horizontal tension force remains the same with altitude. The vertical force increases as:

$$(40) \quad T_z = T_x \left(e^{\frac{2(z+z_0)}{H_c}} - 1 \right)^{\frac{1}{2}} = T_x G(z)$$

where z_0 is chosen to give the proper angle at the bottom of the cable.

The tension in the sheath is proportional to the change in vertical height. This force may be relieved by cables running diagonally off the track/rotor system. The cables deflect the rotor down and make horizontal forces that relieve the tensile forces in the sheath.

For example, assume a stress relief anchor cable from 70 km altitude, and that $z_0 = 20$ km and $H_c = 80$ km for this cable. This implies $T_z = 2.91 T_x$. The force vector points down at an angle of 19° from the vertical. Assume that the sheath/rotor is 10° from the horizontal. Rotate the components of the anchor cable force vector, so that they are 9° from perpendicular to the rotor, pulling up-slope. For an angle of 9°, the force perpendicular to the rotor is 6.3 times the tangential force. If the cable must relieve 400 kN (the force of a 10 kg/m sheath with 4 km of vertical travel), the deflection force perpendicular to the rotor is 2.52 MN, causing the rotor to deflect 0.25 degrees.

Anchor cables relieve stress if the angle of the rotor from the horizontal is greater than the angle of the anchor cable from the vertical. This can be expressed as:

$$(41) \quad \frac{dz}{dx} < \frac{1}{G(z)} = \left(e^{\frac{2(z+z_0)}{H_c}} - 1 \right)^{-\frac{1}{2}}$$

If the relief cables come off the sheath continuously, the resulting sheath shape may be described with a continuous equation. The z and x coordinates are used for altitude and surface position on the curved equator. The deflection force per length perpendicular to the rotor is the curvature times $m_r V_r^2$:

$$(42) \quad f = \left(\frac{\frac{d^2 z}{dx^2}}{\left(\left(\frac{dz}{dx} \right)^2 + 1 \right)^{\frac{3}{2}}} - \frac{1}{(R_E + z) \left(\left(\frac{dz}{dx} \right)^2 + 1 \right)^{\frac{1}{2}}} \right) m_r V_r^2$$

This force divides into vertical and horizontal components. Equating these forces to the weight of the sheath and the tension in the cables gives the characteristic shape of the Launch Loop incline sections:

$$(43) \quad \frac{d^2 z}{dx^2} = \frac{1 + \left(\frac{dz}{dx} \right)^2}{R_E + z} - \frac{a_g (m_s + m_r) \left(1 + \left(\frac{dz}{dx} \right)^2 \right)^2}{m_r V_r^2 \left(1 - G(z) \left(\frac{dz}{dx} \right) \right)}$$

If the relief cables are brought away from the Loop to the side at angle θ from the plane of the Loop (to absorb sideways wind forces, for example), the $G(z)$ term in equation (43) is divided by $\cos(\theta)$. If

$\frac{dz}{dx} = 0$, equation (43) reduces to:

$$(44) \quad \frac{m_s}{m_r} = \left(\frac{V_r}{V_o} \right)^2 - 1$$

This is just the track to rotor mass ratio implied by equation (2).

The ideal incline is short. This implies a steep starting angle. Equation (41) implies a maximum slope, but the vertical height of the lower deflection ramp at the ends sets an even stiffer requirement on the starting angle. The vertical height of the deflection ramp is given by $z_D = R_D (1 - \cos(\alpha_0))$, and is approximately the square of the angle. If the deflection radius is 14 km, a starting incline angle of 20 degrees results in a change in vertical height of 850 m. This ramp can be placed in a floating tunnel below the ocean surface, but that is still quite an engineering feat. A 30 degree deflection ramp changes height by 1880 m; a lot of added expense for a slightly shorter incline.

Assume a rotor mass of 3 kg/m and a track and an incline sheath mass of 10 kg/m. The cables have a

characteristic length H_c of 80 km, and their angle from horizontal at the ground is 39 degrees ($z_0 = 20$ km). They are angled at 45 degrees from the plane of the Loop. Figure 8 shows the results:

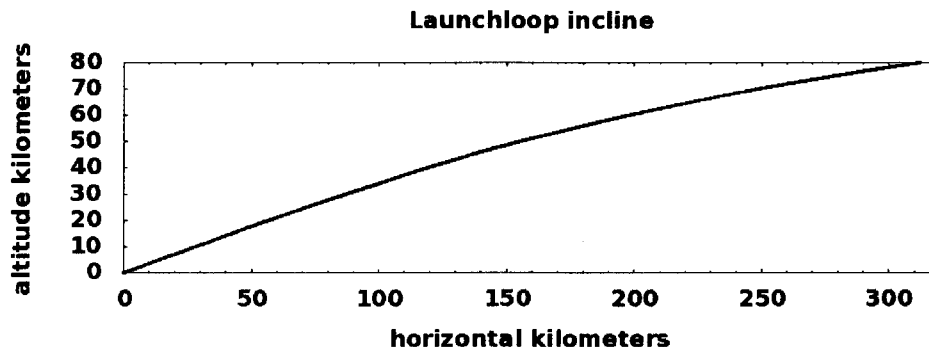


Figure 8. Altitude versus horizontal distance for a typical incline section.

Incline summary table

parameter	bottom value	top value	units
incline sheath mass		10	kg/m
cable angle	38.85		degrees
cable offset	20.0		kilometers
cable support length		80.0	kilometers
incline slope	0.3640	0.1400	vert/horiz
incline angle	20.00	8.01	degrees
deflection force	205,016	82,093	kiloNewtons
deflection force vertical	201,902	81,893	kiloNewtons
deflection force horizontal	35,601	5,731	kiloNewtons
rotor mass density	2.9882	3.0000	kg/meter
rotor velocity	14,055	14,000	meter/sec
gravity	9.81	9.57	meter ² /sec
horizontal distance		311.9	kilometers
vertical distance		80	kilometers
cable force ratio G(z)	1.14	4.73	vert/horiz
top cable axial force		27,701	kiloNewtons / rotor
station support force		54,792	kiloNewtons / rotor
station + elevator mass		5726	metric tons / rotor
main diagonal cable mass		2150	metric tons / rotor
incline cable mass		1280	metric tons / rotor

made with the program launchloop/incline/in01.c version 2009-July-21

The eastbound and westbound rotor segments travel similar paths, and both support the stations, so many of the numbers above are doubled. The total station and elevator mass may be as much as 11,452 metric tons, for example. There are stations at the east and west end, and the west end is busy with launching, while the east end performs observations, rotor maintenance, and emergency support operations.

The curve can be straightened somewhat, and the lower deflector simplified, if the upper end of the incline is constructed more lightly than the lower end. Air pressure and upper altitude winds are mostly gone above 40 km or so, while the curvature-causing vertical-to-horizontal force ratios in the relief cables increase. Lighter sections mean less curvature, permitting a smaller starting angle.

13. Incline Sheath Construction

The incline sections are surrounded by two sheaths to protect the moving rotor from the atmosphere. The outer sheath must be able to maintain high vacuum against mechanical stresses and diffusion from sea level atmosphere. A 14 cm outside diameter allows a large vacuum channel to the nearest pump. The sheath is made with Teflon-coated Kevlar fabric and epoxy-impregnated carbon fiber hoop spreaders spaced 10 cm apart. The outer sheath is covered with a Kevlar-mylar fabric, coated on the inside with 100 microns of metal, making it impermeable to gas diffusion.

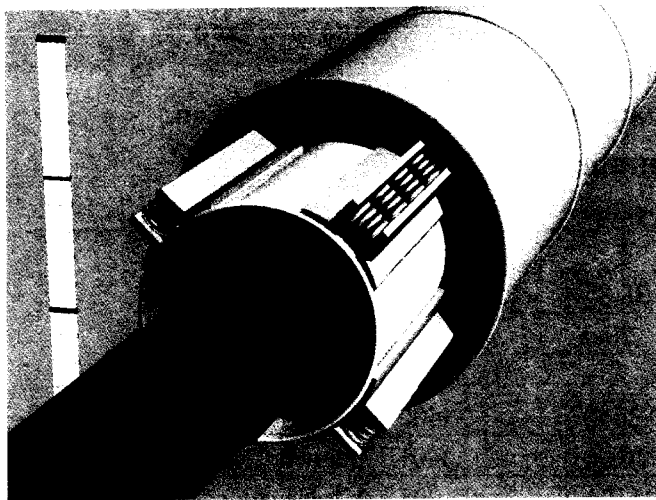


Figure 9.

Cross section of the incline sheath

14 cm diameter

ruler in centimeters

surfaces will actually be black for

high thermal emission

The inner sheath must withstand full atmospheric pressure if the outer sheath is breached. It is made of 2mm thick metal. Since the metal can get very hot, re-radiating the rotor heat, it may need to be made of titanium or another heat-resistant metal.

The sheath weight of 100 N/m, plus wind loadings up to 50 N/m, are transmitted to the rotor with magnets with a lift-to-weight ratio of 3. The resulting magnet weight is approximately 5 kg/m. Much better magnets may be possible.

The inclines may be struck by lightning. A lightning stroke can carry currents of up to 100,000 amps [15]. This current is carried by the outer and inner sheath, and the support cables, to the ground. The pulse propagates in both directions along the sheath. To keep the current from flowing all the way up to the station, the sheath is insulated at 30 km altitude (above the charge center of storm clouds).

The aluminum inner sheath has an electrical resistance of 2.5 m Ω per meter, so 130 volt-per-meter drops can be expected along the inner sheath from a lightning current pulse. The sheath below 10 km altitude is 30 km long. The voltage drop can exceed 4 million volts. Controller interconnections must be designed with this in mind. Some of the lightning discharge current must be conducted to the rotor, to induce a similar voltage drop there, or arc-overs will occur. A lightning stroke transmits a negative charge to the



ground, so the current to the rotor may be transmitted by thermionic cathodes inside the sheath. Since cathode current emission densities of only 3 amp/cm² can be expected [16], a few hundred amps in the rotor must be sufficient to induce voltage drops of 130 volts per meter. This implies a high longitudinal resistance (over large distances) in the rotor, and affects rotor design.

14. Acceleration Track

The launch track and sheath system cover the prograde rotor between the east and west stations. The weight of the launch track and sheath, plus that of the anchor cables, must be equivalent to 7.1 kg/m to put the proper curve on the system. The mass budget for the track/rotor system per meter is:

Temporary deployment sheath	700 g/m
Magnet structures	2400 g/m
Electronics, etc.	300 g/m
Other track weight	600 g/m
Kevlar® cable weight	1000 g/m
Other cable weight	2100 g/m
Total	7100 g/m

Figure 10: Passenger capsules, magnet-wings, and apogee kick motors traveling up the 80km west elevator. (altitude compressed 80x, cables exaggerated 100x for visibility)

15. Elevator to West Station

Vehicles are launched from west station, 80 kilometers above the surface. A fully utilized launch loop may launch 600 metric tons of vehicle and magnet mass per hour. Logistics to and from west station may account for another 100 tons per hour from the ground to west station and back. The elevators to west station (two main cable-and-pulley powered lift elevators, along with support cable emergency descent vehicles) are the main logistical connection to the floating west end surface station.

The surface station has a floating runway, hangars, warehouses, and docks; a small floating city. It is hundreds of kilometers from the west end turnaround, and from the main west end anchor cables.

The elevator vehicles are un-powered, and propelled by forces in the elevator cables supplied by pulleys and large electric motors. The lift cables have multiple sections, so that they can rapidly accelerate and decelerate one elevator vehicle at a time. Lifting a net 600 tons vertically to west station per hour requires a mechanical power level of 130 Megawatts - fortunately, these monstrous motors can be on the surface, and power provided to all the rotating cables mechanically.

The cable system has three sections - a lower acceleration section from 0 to 4 kilometers altitude, a middle lifting section from 4 kilometers to 72 kilometers altitude, and an upper deceleration/coasting section up to west station. In the lower section, elevator vehicles are accelerated at 20 meters per second squared for 20 seconds, reaching 400 meters per second at 4 kilometers altitude. The 20 m/s^2 is added to the gravitational acceleration of 9.81 m/s^2 ; the payloads must endure 3.1 gees during this time. At 2900 meters altitude, the elevator vehicles pass 343 meters per second, the speed of sound. This will likely generate a sonic boom and a Prandtl-Glauert vapor cone.

16. Launch Loop Failure

Catastrophic failure of the Loop can be expected occasionally because of control failure, fatigue, weather, improper vehicle handling, or major breaks in the sheath. It is important that the rotor can be dumped from the track in a way that is not damaging to the structure or to the environment. 1.5×10^{15} Joules is enough energy to boil 400,000 m^3 of seawater. This is equivalent to 30,000 tons of burning oil, or about 10% of the capacity of a modern supertanker. For safety reasons, Launch Loops must not be constructed near populated areas.

Most of the rotor will be dumped into the ocean. Some of it may escape at high altitude. With its very high velocity, it will leave the atmosphere and then the region around the Earth, and go into elliptical solar orbits. Depending on the time of day of the failure, eastbound and westbound rotor segments will travel in solar orbits of varying inclination and ellipticity. It is unlikely that the segments will stay together, so they will be isolated, 2 meter long, 6 kilogram cylinders traveling in a loose swarm.

These errant rotor fragments will share most of the Earth's 30km/s orbital speed. They will not fall into the Sun, and probably won't come near Venus or Mars. They will orbit the sun for a very long time. Since their orbits will be unlikely to have periods that fractionally relate to a year (for example, $14/17$ ths of a year), the coincidences when an integral number of fragment orbits correspond to an integral number of earth revolutions (when they are in the same plane) will be few. This means they will be in orbit for a very long time, perhaps millions or billions of years, before they collide with the Earth, hopefully disintegrating and burning up in the atmosphere.

The rest of the Launch Loop should survive for reuse. There should be provisions for parachutes on the upper deflection stations and portions of track and cable, so that these may be recovered if the Loop falls down. Lastly, spares for everything that can fall should be kept on hand, to minimize reassembly time. These measures will increase the operating cost of the Launch Loop, but greatly reduce rebuild costs and down-time.

17. Collisions with Space Junk

Meteoroids and orbiting space debris can collide with and break the Launch Loop track. Meteoroids come from random directions, and are not often in circular Earth orbits; the Loop has only one chance to collide with them before they fall below it. The flux rate of particles large enough to seriously damage the Loop is too low to pose a hazard [11].

Orbiting space debris from human activity in space is in a decaying, near-circular orbit by the time it reaches Launch Loop altitudes. Orbiting debris has many chances of collision, it poses a greater threat.

Assume that there is a steady "rain" of debris objects with mass M_d , effective drag area A_d and collision radius $R_d \approx \sqrt{A_d}$ spiraling in from nearly circular orbits at a rate of N_d . The atmospheric drag on an object is given by the form drag, which results in a power loss of:

$$(44) \quad \frac{\partial E}{\partial t} = 0.5 \rho_A A_d V_o^3$$

This energy loss lowers the orbital altitude over time. The change of energy with altitude h is given by:

$$(45) \quad \frac{\partial E}{\partial h} = 0.5 M_d a_g h$$

where a_g is the gravitational acceleration. The change in altitude with time can be derived as:

$$(46) \quad \frac{\partial h}{\partial t} = \frac{A_d \rho_A V_o^3}{M_d a_g}$$

R_s is the radius of the track and rotor. All objects between $(R_d + R_s)$ and $-(R_d + R_s)$ can potentially hit one of the two tracks. Thus, the number of objects N that *might* hit the Loop are in a shell $4(R_d + R_s)$ thick; that number is:

$$(47) \quad N = 4(R_d + R_s) \frac{\partial t}{\partial h} N_d = \frac{4(R_d + R_s) M_d N_d a_g}{A_d \rho_A V_o^3}$$

Each of these objects crosses the equator twice per orbit, at a velocity V_o , independent of orbital inclination. The flux rate past the equator is thus:

$$(48) \quad \frac{d N_E}{d t} = \frac{N V_o}{\pi R_E}$$

where R_E is the radius of the Earth. An equatorial Loop intercepts a fraction of these proportional to its length:

$$(49) \quad \frac{d N_L}{d t} = \frac{L_{LOOP}}{2 \pi R_E} \frac{d N_E}{d t}$$

The resulting collision flux is:

$$(50) \quad \frac{dN_L}{dt} = \frac{2(R_d + R_s)L_{LOOP}M_d N_d a_g}{A_d \rho_A \pi^2 R_E^2 V_o^2}$$

The form of equation (50) suggests that after a given amount of mass *MMTF* (Mean Mass To Failure) passes through the altitude of the Loop, there will be a collision. Using the identity $V_o^2 \equiv R_E a_g$,

we can take the inverse of equation (50) to get the *MMTF* :

$$(51) \quad MMTF = \left(\frac{A_d}{1 + R_d/R_s} \right) \left(\frac{\rho_A \pi^2 R_E^3}{2 R_s L_{LOOP}} \right)$$

Debris object parameters in the left factor, Launch Loop and atmospheric factors in the right factor. The worst case problems are caused by small dense objects (low A_d) which will travel a larger fraction of an orbit before plummeting. Remember that *all* objects in orbit around the Earth cross the equatorial plane twice per orbit, and most Launch Loops will be near the equator.

Assume that a typical piece of space debris is a bolt with a drag area of 1 cm² and a radius of 1 cm. For a Loop at 80 km altitude, the orbital radius is 6450 km and the atmospheric density is 1.9E-5 kg/m³.

The Loop radius is 5 cm. The result is a *MMTF* of 2E7 kg or 20,000 tonnes. While this seems like a large amount, remember that one Launch Loop system at full power can launch that much mass into space in two days.

The high launch rates allowed by the Launch Loop requires that users act responsibly and not litter the regions of space near the Earth. The low launch costs of the Launch Loop will make garbage collection missions affordable. Users will have no excuse to leave radar detectable fragments in orbit, and will be liable if they do.

18. Drag Effects in Near-Earth Space

A major loss in the Launch Loop system is gas drag on the moving surface of the rotor. Gas drag on the vehicle is also a problem, requiring vehicle launches at slightly higher velocity than would otherwise be necessary. This drag is the main reason the launch path is elevated to high altitudes.

A very thin, pumped sheath surrounds the rotor, with pumping stations spaced at 10 km intervals along the launch track. This sheath allows the rotor to move in a very high vacuum. Because the sheath is thin, it is easily punctured by meteoroids and debris, and ambient air can pour through a breach into the sheath. Fortunately, the movement of the rotor helps move gas from a breach to the nearest pumping station.

A major breach may be as large as the cross sectional area of the sheath, about 20 cm². The air pressure at 80 kilometers altitude is 0.11 Pa, and the density is 1.9E-5 kg/m³ [17]. Gasses flow through this breach at a pressure-driven rate of $A\sqrt{2\rho P}$, or 4.1E-6 kg/s. Gasses move down the sheath at V_a , dependent

on internal sheath structure. If $V_a \approx 0.25 V_r$, there is about 6E-10 kg of gas per meter of sheath, yielding a gas density of 6E-7 kg/m³ inside the sheath. The mean free path is approximately 20 cm, justifying a free-molecule treatment of the problem.

Assume a worst-case wall accommodation coefficient of unity; that is, all molecules scatter from impacting the rotor or sheath. The skin friction on the rotor (with a long mean free path) is given by the particle flux rate times the energy gained per particle collision [14]:

$$(52) \quad Power \approx \frac{A \rho_A (V_r - V_a)^2 V_{th}}{(24\pi)^{1/2}}$$

Assume the thermal velocity V_{th} is 5000 m/s, the energy per molecule is 4 eV and the equivalent temperature is 30,000K, heated by friction.

If pumping stations are spaced at 10 km intervals, up to 1000 m² of rotor may be exposed. The drag loss from equation (52) is 40 MW. This heats the rotor by 1.6K. While such a major breach should be sealed to save power, it will not cause the Launch Loop to fail.

Even if the sheath is not breached, the normal ambient gas density in the sheath causes drag. If the gas pressure is 0.01 Pa, and the gas temperature is 30,000K, the gas density in the sheath is 1.2W-9 kg/m³ and the drag loss on 5.2E5 m³ of rotor is 40 MW. While much better vacuums are possible, there is a tradeoff between pump cost and power cost.

A more important problem may be sputtering, or hypervelocity spalling cascades. If an iron atom is knocked loose at 14 km/s, it has an energy of 60 eV when it hits the sheath wall. This may be enough to sputter loose another atom, which collides with the rotor, and so forth - the result may be a cascade of particles. For this reason, it is a good idea to coat the rotor and the sheath wall with a material with low atomic weight and a low sputter yield. Coating the surfaces with pyrolytic carbon, for example. This would be strong (in the direction of low-angle glancing collisions) and low molecular weight, if it does get broken loose.

19. Vehicle Atmospheric Drag

Atmospheric drag on the vehicle causes power losses, and requires a higher terminal velocity on the vehicle to punch through what remains of the atmosphere.

For a vehicle with an effective frontal area of A_p and air density ρ_A , vehicle drag power is given by:

$$(53) \quad Power = 0.5 \rho_A A_p V_p^3$$

Integrated over the launch path, this yields the lost drag energy E_{D0} :

$$(54) \quad E_{D0} = \frac{\rho_A A_p V_p^2 L_{LOOP}}{4}$$

After the vehicle leaves the Loop, it climbs out of the atmosphere in an elliptic orbit. The drag acceleration a_D as a function of altitude is:

$$(55) \quad a_D = \frac{\rho_0 e^{-z/H_A} A_p V_p^2}{2 M_p}$$

The altitude as a function of horizontal distance is:

$$(56) \quad z = \frac{x^2}{2 R_E} \left(1 - (V_o/V_p)^2 \right)$$

The equations can be combined and integrated to yield:

$$(57) \quad E_{Dl} = \frac{(2 \pi R_E H_A)^{half} \rho_0 A_p V_p^2}{4 \sqrt{1 - (V_o/V_p)^2}}$$

Assume a vehicle weighing 5000 kg with an effective frontal area of 2 m² is launched to a velocity of 10,500 m/s. The atmospheric drag forces from an 80 km launch result in a deceleration of 0.5 m², and energy losses of 0.8% on the Loop and 0.5% on the way out of the atmosphere. These are acceptable losses. A launch track at higher altitudes reduces losses, but is exposed to more space debris.

20. Launching Vehicles

Destination	Launch V m/s	2000km gees	2000km time s	10gee dist km	10gee time s	transit hrs	Arrival ΔV m/s	altitude km	radius km
LEO	7451	1.41	537	283	76	0.74	65	300	6678
m288	8586	1.88	466	376	88	1.30	1009	6411	12789
GEO	9875	2.49	405	497	101	5.24	1490	35786	42164
Moon	10547	2.84	379	567	108	119.42	833	378022	384400
Slingshot Moon to m288	10547	2.84	379	567	108	241.74	-2184	6411	12789
Slingshot Moon to GEO	10547	2.84	379	567	108	255.56	-1053	35786	42164

6378+80km launch altitude, 471m/s eastward boost, 1gee=9.81m/s

Slingshot orbits around the moon take a long time to reach m288 and GEO, and have a narrow launch window to reach the right position and velocity for slingshot boosting to occur. However, the arrival ΔV has the opposite sign from transfer orbits directly from earth. This permits the use of rotating capture tethers intermediate orbits, averaging the velocity and momentum of payloads arriving from the two different routes, and eliminating the need for large apogee kick rocket motors for orbit circularization.

A typical five-metric-ton vehicle is shown in Figure 11. The vehicle is equipped with rocket engines for orbit circularization at apogee arrival, a lifting shell, and a heat shield and parachutes for emergency reentry of passengers. Magnets hold the vehicle off the rotor using eddy current repulsion. Cheaper

containers may be used for expendable cargo. They may even be launched on fortified wooden pallets! There will still need to be apogee kick motors, and provisions to re-enter the re-usable magnet racks.

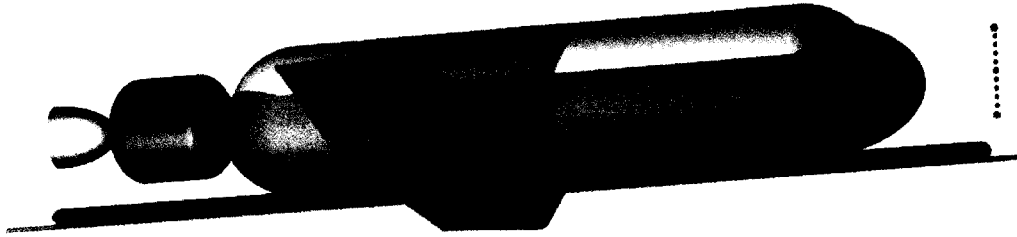


Figure 11. A typical 5 ton passenger capsule, with magnet rack, rocket motor for apogee orbit insertion, and wings and a heat shield for accidental reentry. Scale is 1 meter.

The 10 meter long magnet rack on the vehicle generates a lift force of 50 kN and a drag force of 150 kN on the rotor, which holds the vehicle up against gravity and accelerates it at 3 gees. With the vehicle near rest velocity, the rotor is decelerated 3.6 m/s, and deflected downwards 1 m/s, an angle of 90 micro-radians. As the vehicle accelerates, the speed relative to the rotor drops, decelerating the rotor by 14 m/s at a vehicle speed of 10.5 km/s.

Tension must be released on the station anchor cables at either end of the launch track to compensate for the weight of the vehicle. At the beginning of acceleration, the 90 micro-radians of deflection under the vehicle is matched by a reduction of 90 micro-radians at west station. As the vehicle moves east, the west station deflection increases and the east station deflection decreases. As the vehicle approaches orbital velocity, the sum of station deflections increases, since the Loop is supporting less vehicle weight.

The deflection of the rotor and track is illustrated in Figure 12. The following analysis is performed in the vehicle's frame of reference.

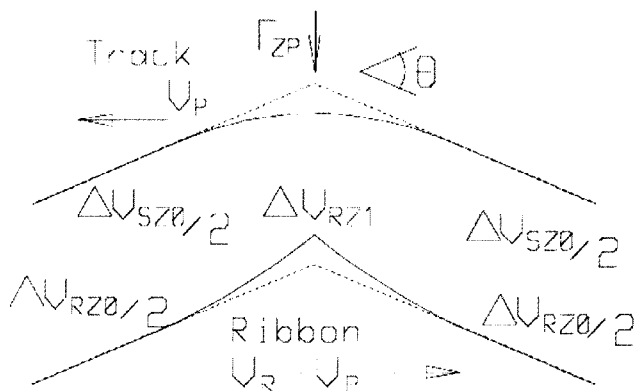


Figure 12.

The deflection of rotor and track as they pass by the vehicle.

Defining V_o as the circular orbit velocity, the downwards impulse force on the rotor, and indirectly on the track, is given by:

$$(58) \quad F_p = a_g M_p \left(1 - (V_p / V_o)^2 \right)$$

Under the vehicle, this force is absorbed by a vertical rotor velocity change of ΔV_{rz} . The velocity change is:

$$(59) \quad \Delta V_{rzl} = \frac{F_{zp}}{m_r (V_r - V_p)}$$

The track is uncoupled from the vehicle. It experiences no sudden change in velocity, but is accelerated by the control magnets to match the rotor. This results in a vertical change in rotor velocity of ΔV_{rz0} , and ΔV_{sz0} for the track. The velocities are related by the angle θ that the track is deflected:

$$(60) \quad \theta = \frac{\Delta V_{rz0}}{V_r - V_p} = \frac{\Delta V_{sz0}}{V_p}$$

The force is given by:

$$(61) \quad F_{zp} = m_r \Delta V_{rz0} (V_r - V_p) + m_s \Delta V_{sz0} V_p$$

Define the track mass parameter $\mu \equiv m_s / m_r$. Solving for ΔV_{rz0} and ΔV_{sz0} :

$$(62) \quad \Delta V_{rz0} = \frac{F_{zp} (V_r - V_p)}{m_r ((V_r - V_p)^2 + \mu V_p^2)}$$

$$(63) \quad \Delta V_{sz0} = \frac{F_{zp} V_p}{m_r ((V_r - V_p)^2 + \mu V_p^2)}$$

The change in velocity is the result of control magnet forces between track and rotor over a horizontal region x_c to each side of the vehicle. The force in this region is a fraction χ of the track-to-rotor attraction force. χ is limited in one direction because the track and rotor cannot repel each other ($\chi > -1$). In the other direction, χ is limited by the maximum force the control magnets can generate, and the peak power the power control devices can handle.

Since the track and the rotor do not follow the same path, the spacing between them changes. If the spacing becomes too great, the control magnets are unable to compensate, and the system falls apart. If the spacing becomes zero, the track crashes into the rotor.

The spacing change is a function of vehicle mass and velocity, and track and rotor mass per length. For a given maximum spacing change and vehicle mass, there is a minimum rotor mass. This one consideration scales the mass of the rotor, and indirectly the rest of the Launch Loop.

Define the two variables $\alpha \equiv V_r / V_o$, and $\beta \equiv V_p / V_o$. The length of the region disturbed by a payload passage can be expressed as:

$$(64) \quad \Delta x = \frac{1}{\chi} \left(\frac{M_p}{M_r} \right) \left(\frac{\beta^2 (1 - \beta^2)}{(\alpha - \beta)^2 + \mu \beta^2} \right)$$

and the change in vertical spacing is:

$$(65) \quad \Delta z = \left(\frac{M_p}{m_r} \right)^2 \left(\frac{a_g}{8 \chi V_o^2} \right) \left(\frac{\beta}{\alpha - \beta} \right)^2 \left(\frac{(1 - \beta^2)^2}{(\alpha - \beta)^2 + \mu \beta^2} \right)$$

There is a vehicle velocity V_p between 0 and V_o where equation (65) is maximized. This is the velocity at which the rotor is pulled farthest from the track by a payload passage. Given $\mu=2.0$ and $\alpha=1.75$, the equation is maximized with a $\beta \approx 0.658$. The maximum deflection for the parameters given is:

$$(66) \quad \Delta z_{max} = \left(\frac{M_p}{m_r} \right)^2 \left(\frac{0.0071 a_g}{\chi V_o^2} \right)$$

Given $\chi = -0.5$, a 5 metric ton payload, and a rotor mass of 3 kg/m, the spacing change is -0.5 cm. The disturbance spreads over a 420 meter region of the rotor-track system.

A vehicle traveling faster than V_o generates an upwards force. Almost all of this force is eventually provided by the deflection of the track, requiring a very strong coupling force between the rotor and track. If a 5000 kg payload is traveling at 10.5 km/s relative to the Loop, a χ of 36 is needed to maintain a spacing change of 0.5 cm; that is, 36 times the normal attractive force. The track-rotor region affected is about 40 meters long; the higher force is required for about 5 milliseconds.

The rotor center-of-mass can be modified rapidly with small spring-loaded “cock and release” counterweights below the track. If these weigh 5% of track weight, and can be fired at 24 meters per second, they will change the sheath/magnet velocity by the necessary -1.2 meters per second. Rather than springs, the counterweights may be fired by solenoid coils connected to other solenoid coils just beneath the vehicle magnets - the passage of the vehicle provides the energy and momentum to rapidly fire the counterweights. With techniques such as these, the track controller impulse power can be greatly reduced.

The passage of the 10 meter long vehicle support magnet also induces oscillations in the rotor segments. As the forward end of a segment passes into the magnet field, it slows before the back end does, compressing the segment. When the compression wave reaches the back end of the segment, it is reflected as a tension wave, and the segment oscillates. A similar tension wave is started when the segment passes the front of the vehicle. This second wave can add constructively or destructively to the previously generated wave. The stretch in the segment is worst when the speed difference between vehicle and rotor is the speed of sound in the rotor material, which occurs when the vehicle speed is about 6 km/s. The speed of sound in the rotor material is C , the magnet length is L_M , and the segment length is l_{seg} . The maximum compression or stretch in the rotor is:

$$(67) \quad stretch = \frac{a_p M_p l_{seg}}{2 m_r L_M C^2}$$

This value of stretch occurs if the end effects add constructively. For the current design, the maximum segment stretch is 0.014%. This effect can be minimized by making L_M an even multiple of l_{seg} , so that the waves add destructively.

Sudden introduction of vehicle forces on the rotor at west station can also have a bad effect on the rotor. A sudden slowing down of the rotor affected by the vehicle can make it separate from the rotor ahead of it. The vehicle acceleration should be increased gradually to prevent this. If the payload force is increased from zero to $a_p M_p$ over time t_s , and L_L is the length of the Launch Loop from the west station to the east motor, the total stretch of the rotor is:

$$(68) \quad stretch = \frac{a_p M_p L_L}{m_r V_r^3 t_s}$$

Ten seconds is allowed to change the acceleration from 0 to 30 m/s². The rotor velocity change of 3.6 m/s is spread over 140 km of rotor. This results in a 0.4% stretch by the time the rotor reaches the motors at the east end, where the velocity is restored. The rotor may be "pre-accelerated" by the east end motors in anticipation of a payload launch, cutting the stretch in half.

The easiest way to make this gradual load increase on the rotor is by providing initial acceleration to the vehicle at west station with a 1500 meter electromagnetic catapult. This may be a mostly passive system, with inverse induction motor coils picking sinusoidal power off the rotor then applying it to much more widely spaced coils on a track at west station. By monitoring currents, voltages, and fluxes along this catapult, the behavior of the magnet-wing may be characterized and the vehicle launch aborted if dangerous anomalies appear.

A problem can also occur at the east end of the launch path, as the vehicle is nearing rotor speed. The rotor is decelerated by up to 15 m/s; to get this portion of the rotor back up to speed requires a power input of 9 gigawatts. If the velocity change is spread out over the rotor to minimize stretch, the affected section of rotor may be brought up to speed by multiple passes through the motors.

Vehicles can also be launched in "burst mode". Velocity changes are averaged out over the rotor if vehicles are launched in rapid succession and at just the right rate. The entire rotor may be slowed perhaps 50 m/s by such a burst. The support capability of the rotor is lowered by only 1%, causing the cable tension at the surface to drop about 30%. A rotor ΔV of 50 m/s can launch a burst of 15 vehicles in 6 minutes. The velocity may be restored slowly with low power motors.

21. Rotor Cooling

Vehicle drag results in ohmic heating of the rotor. The heat is stored in the rotor and carried away from the vehicle, then dissipated by black body radiation from the hot rotor to the inner sheath wall. The heat

removing capacity of the rotor is proportional to $V_r - V_p$ (that is, rotor - payload) and decreases with vehicle speed; fortunately drag dissipation is proportional to the same factor. If the rotor heats up past the Curie temperature of iron, 1000K, it stops behaving as a magnetic material, and the control magnets fail. Vehicles should not be launched faster than the rotor can cool itself.

The temperature change of the rotor as it passes under the vehicle is:

$$(69) \quad \Delta T = \frac{a_p M_p}{2 \pi R th \rho_{Fe} HC_{Fe}}$$

where $R=2.5\text{ cm}$ is the radius and $th=0.24\text{ cm}$ is the wall thickness of the round iron rotor, which has a density of ρ_{Fe} (7880 kg/m^3) and a heat capacity of HC_{Fe} (600 J/kg-K). A five ton vehicle accelerating at 3 gees changes the rotor temperature by 84K.

The rotor thermal dissipation per length is given by:

$$(70) \quad \frac{\partial P}{\partial x} = 2 \pi R \epsilon \sigma_B (T_r^4 - T_s^4)$$

where ϵ is the emissivity and σ_B is the Stephan-Boltzmann black body constant ($5.67\text{E-}8\text{ W/m}^2\text{ K}^4$).

T_r is the rotor temperature and T_s is the background temperature. If the power dissipation for the 2600 km rotor is 350MW, ϵ is 0.8, and T_s is 250K (average temperature at the 80 km mesopause) the average rotor temperature is 390K.

Over time, the heated rotor radiates and cools. The change in rotor temperature with time is given by:

$$(71) \quad \frac{dT_r}{dt} = - \left(\frac{\epsilon \sigma_B}{\rho_{Fe} HC_{Fe} th} \right) (T_r^4 - T_s^4) \approx 4\text{E-}12 T_r^4$$

The rotor sheds heat much more efficiently at high temperatures. Near 900K, the rotor temperature drops 84K in 45 seconds. If the temperature is limited to 900K, this places a **thermal limit** of **80** evenly-spaced 5 ton lunar payloads per hour on this size of Launch Loop. Larger diameter, heavier rotors can dissipate more heat. Smaller payloads will have lower temperature spikes. so divisible payloads (microsats, consumables) should be launched in frequent small packages.

Early Launch Loops may have a lower thermal limit set by the sheath materials chosen. The sheath must re-radiate the heat it absorbs from the rotor, and could get quite hot during burst launches. Permanent magnets may exceed their upper temperature limits, sensors may be damaged, and the electronics should be located where it can radiate heat well away from the rotor and sheath.

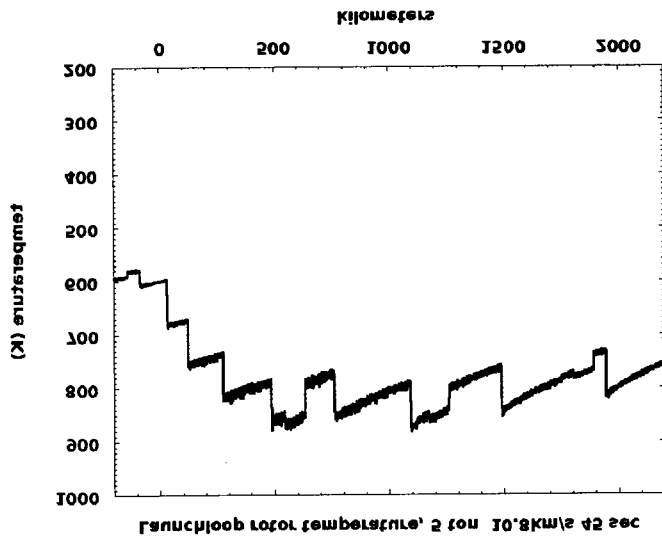


Figure 13: Temperature profile of Launch Loop rotor during continuous launch. A simulation of Equations 69 and 71 for 5 ton payloads launched to 10800 m/s:

Figure 14. Temperature profile of the Launch Loop rotor during a 15-vehicle, 24-second-spaced burst mode launch is graphed in Figure 14. The temperature reaches nearly 900K. Another such burst cannot be repeated for half an hour, although shorter bursts can be more frequent.

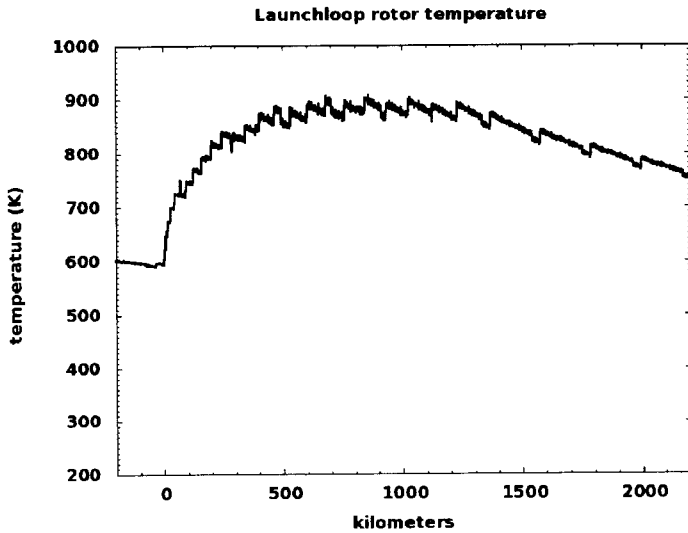
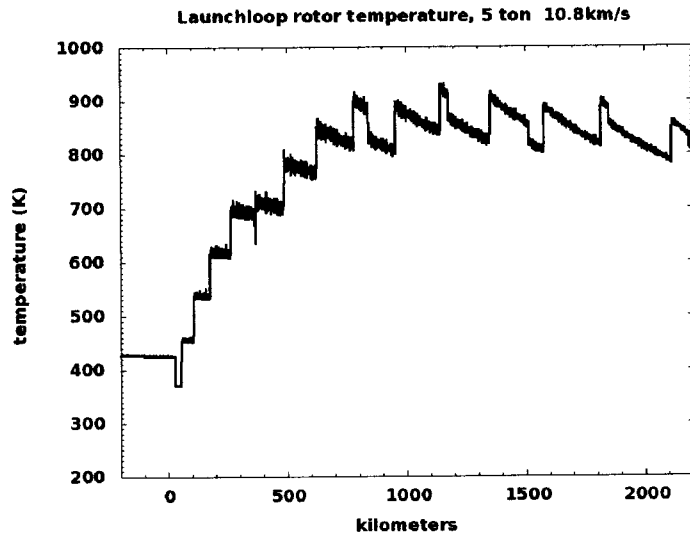


Figure 15.

Temperature profile of the Launch Loop rotor for 1.6 ton vehicles every 10 seconds to 6411km altitude.

At this rate, with a 60% payload fraction at apogee insertion, we can deliver 3 million tons to m288 per year.

22. Energy and Power Use by the Launch Loop

The vehicle is accelerated by rotor drag, and the total kinetic energy removed from the rotor is more than twice the resultant vehicle kinetic energy. A 5 ton vehicle launched at 10.5 km/s removes 735 GJ of kinetic energy from the rotor, slowing it down by 3.6 m/s at the start of acceleration and 14.3 m/s at the end. This energy is put back in by a high-efficiency linear induction motor located on the surface near the eastern turnaround. This motor is driven by a 150 kHz source and is 10 km long, with 1 million ferrite cores for poles. The motor supplies power to the rotor which in turn drives the generators on the low acceleration section magnets; it also makes up for drag caused by residual gasses in the sheath.

The track magnet power consumption is about 40 MW, and the deflectors consume about 100 MW. Drag from residual gasses and magnetic field discontinuities consumes about 60 MW. If a 500 MW power generator is available, then 300 MW is available for restoring losses from vehicle launches. This allows the launch of 35 five-ton vehicles per day to near escape velocity, or 48 per day to low earth orbit.

To launch at maximum rate, a much larger power plant is needed. Launching 5 ton vehicles to near-escape velocity at the high rate of 80 per hour requires a 17 GW power plant. This one smaller Launch Loop can serve two very different sized launch markets.

The power from the generators is put into the rotor of the Loop with 10 km long, high-efficiency linear induction motors. The motors may be analyzed like those planned for high-speed surface trains [10]. Launch Loop motors are longer, narrower, higher power, and much higher velocity, resulting in efficiencies approaching 100%. The short motor wavelengths and high speed requires high frequency, switched-mode power supplies. This results in more costly drive electronics than the line-frequency power switches used for normal motor applications. The costs and driver efficiencies are similar to those of large, high-efficiency switched power supplies.

23. Construction and Operating Costs

A detailed estimate of the costs involved is premature. Some costs can be identified, or compared to existing construction projects. The following crude estimate does not include the cost of apogee insertion motors, payload shrouds, communication packages, or other per-vehicle costs. Nor does it include the reduction in useful payload weight caused by the weight of these items.

600 metric tons carbon fiber at \$25/kg	\$ 15M
6000 metric tons Kevlar® aramid fiber at \$25/kg	\$150M
1500 metric tons Alnico 8, at \$40/kg, formed	\$ 60M
500 MW motor power switchers	\$ 50M
1 million ferrite motor cores, at \$3 each	\$ 3M
470,000 low power track controllers, at \$100 each	\$ 47M
50,000 high power track controllers, at \$1000 each	\$ 50M
150,000 D magnet controllers, at \$800 each	\$120M
Total	\$572M

(\$100 per control package and \$0.10 per average watt assumed) - reall y old numbers!

Other costs can be identified, such as sheath manufacturing, magnet winding, ramps, pumps, and so forth. The cost of floats and anchoring cables to the seabed are unknown.

Assume the total cost of the Launch Loop, including research costs, comes to 2 billion dollars. If it is used at only 30% capacity of 500 MWe (26,000 metric tons per year), and is amortized over 1 year as a high-risk venture, the cost per gross kilogram (including 6 cents per kWh oil fuel cost) is \$85. While this launch rate is nearly two orders of magnitude above present U.S. launch rates, it is a tiny fraction of the 3.5 million tons per year capacity of the basic system.

Later, at 85% usage of a 4 GWe power capacity (750,000 tons per year), 5 year amortization, 9 billion dollar capital cost, and 1.3 cents per kWh fuel cost, the cost per gross kilogram is \$3. At this cost, labor and vehicle systems will probably dominate net payload cost.

Total Launch Loop system cost is likely to be well below that of Earth-to-high-orbit rocket systems.

24. Possibilities

This version of the Launch Loop launches 5 metric ton vehicles from the Earth to geosynchronous, LaGrange, and lunar destinations. Other applications are possible.

Economics and payloads set Launch Loop throughput, size and speed. The rotor can be made wider or longer. More rotors can be added to the side. Thousands of Launch Loops can be built on the equator.

Increasing the rotor speed of a Launch Loop opens the rest of the solar system. Rotor speeds of 18 km/sec can send vehicles directly to Venus, Mars, the asteroid belt, and Jupiter. Other destinations may be possible with planetary assist maneuvers. Efficiency is low for lower ΔV missions, however.

The present scheme for the Launch Loop includes two expensive and power-consuming 180° deflectors. The deflectors can be eliminated by a Loop that encircles the Earth, brought down to the ground at appropriate intervals, or running entirely in orbit with periodic anchor cables and elevators. Such a launch system must be constructed from orbit [5,6].

Launch Loop technology is useful for other purposes. The low ratio of dissipation to energy storage make the Loop an effective form of energy storage for power grids, and an interesting method of transmitting power over long distances. Power can be transmitted for 5000 km with less than 1% loss. Similar superconducting ring structures have been considered [14].

Lastly, Launch Loops may be constructed off Earth. A 200 km Launch Loop on the Moon can be operated entirely on the surface, without elevating ramps. Gee forces would be less than present mass driver designs, and the Launch Loop would be easier and much cheaper to construct. Launch Loops can be built on orbiting structures, providing in-space transportation without expending reaction mass, if traffic in all directions is properly balanced. Passive capture rotors can be placed on orbiting structures for capturing material launched from Earth and Moon.

Conclusions

More study remains to determine the details of a Launch Loop operation; the idea may prove impractical because of instabilities, expense, or political obstruction. Regardless of its success, it is hoped that others are stimulated to think of low-cost approaches to Earth launch using existing physics and existing engineering materials.

The rocket has served us well during the last few decades, and will continue to find uses in new applications and at the frontiers of space. The paying traffic justifying even a minimum scale Launch Loop must be established before its construction. Rocket launch vehicles are establishing this market. Low-cost space utilities such as the Launch Loop will replace rockets in high volume applications, making space settlement and industrialization economically practical.

References

- [1] Future Space Transportation System Study, *Astronautics and Aeronautics*, Vol. 21, June 1983, pp. 36-56.
- [2] Chilton, F., Hibbs, B., Kolm, H., O'Neill, G. K., and Phillips, J., Electromagnetic Mass Drivers, *Space Based Manufacturing from Nonterrestrial Material*, AIAA Progress in Astronautics and Aeronautics, Vol. 57, 1977, pp. 37-61.
- [3] Kolm, H., "Mass Driver Up-Date," *L-5 News*, Vol. 5, Sept. 1980, pp. 10-12.
- [4] Arnold, R., and Kingsbury, D., "The Spaceport," *Analog*, Vol. 99, Nov. and Dec., 1979.
- [5] Brakke, K., "The Skyrail," *L-5 News* July, 1982.
- [6] Birch, P., "Orbital Ring Systems and Jacob's Ladders," *Journal of the British Interplanetary Society*, Vol. 35, November 1982, pp. 475-497.
- [7] Moravec, H., "A Non-Synchronous Orbital Skyhook," *Journal of the Astronautical Sciences*, Vol. 25, No. 4, 1977.
- [8] Atherton, D. L., "Maglev Using Permanent Magnets," *IEEE Transactions on Magnetics*, Vol. MAG-16, Jan. 1980, pp. 146-148.
- [9] DuPont Bulletin K-2, "Characteristics and Uses of Kevlar™ 49 Aramid High Modulus Organic Fiber," DuPont Textile Fibers Department, Technical Service Section, Wilmington, Delaware 19898.
- [10] Yamamura, S., *Theory of Linear Induction Motors*, Wiley, 1979, 2nd edition.
- [11] Vedder, J. F., "Micrometeoroids," *Satellite Environment Handbook*, Stanford University Press, 1965, 2nd edition.
- [12] Madden, R. A. and Zipser, E. J., "Multilayered Structure of the Wind over the Equatorial Pacific During the Line Islands Experiment," *Journal of the Atmospheric Sciences*, Vol. 27, March 1970, pp. 336-342.
- [13] O'Hanlon, J.F., *A User's Guide to Vacuum Technology*, Wiley, 1980.
- [14] Hull, J. R., "Magnetically Levitating Loop, A New Energy Storage Concept," Internal research paper, Argonne National Laboratory, April 1983.
- [15] Uman, M. A., *Lightning*, Dover, 1984.
- [16] *Reference Data for Radio Engineers*, International Telephone and Telegraph Corporation, 1956, fourth edition, p. 367.
- [17] *CRC Handbook of Chemistry and Physics*, 1982, 63rd edition, p. F166.
- [18] Lofstrom, K., "The Launch Loop," AIAA-85-1368, *21st Joint Propulsion Conference*, 1985.

[19] Lofstrom, K., "The Launch Loop," *Analog*, Vol. 103, Dec. 1983, pp. 67-80.

[20] Derksen, Bryan., svg redrawing of launchloop for http://en.wikipedia.org/wiki/Launch_loop

Open Source Software used to create the presentation, paper, and website:

<http://www.libgd.org/> LibGD, a useful collection of 2D drawing primitives.

<http://www.povray.org/> 3D modeling and ray tracing rendering engine

<http://moinmo.in/> MoinMoin wiki software

<http://www.math.union.edu/~dpvc/jsMath/> Rendering math on the web using javascript

<http://wiki.themel.com/jsMathParser> moinmoin plugin for mathgsl

<http://www.gnuplot.info/> The gnuplot graph plotting package

<http://www.gnu.org/software/gsl/> libgsl, The Gnu Scientific (math) Library

Math::GSL at any CPAN repository. Jonathan Leto's Perl implementation of libgsl

<http://www.swftools.org/> SWFtools used for the website animations.

<http://openoffice.org/> it sucks, but less. It is open source, which helps.